

**NASA
Technical
Paper
3675**

1997

A Survey of Theoretical and Experimental Coaxial Rotor Aerodynamic Research

Colin P. Coleman, Ames Research Center, Moffett Field, California



National Aeronautics and
Space Administration

Ames Research Center
Moffett Field, California 94035-1000

Contents

	Page
List of Figures	v
Nomenclature	vii
Summary	1
Introduction.....	1
Definitions	2
Research in the United States of America	2
NACA Langley Research Center	2
De Lackner Helicopters, Inc.	4
Sikorsky Aircraft	5
Research in Russia	7
Research in Japan.....	13
Hover	13
Forward Flight.....	18
Research in the United Kingdom.....	19
Research in Germany	21
Conclusions.....	22
References.....	23

List of Figures

	Page
1 Henry Bright's 1859 coaxial design patent (ref. 1).....	1
2 Scale effect on rotor 1 performance at 327 ft/sec, H/D = 0.093. Lines drawn through data (ref. 3).....	3
3 Effect of solidity on rotor of merit (ref. 3).....	3
4 Comparison of theoretical (solid line) and experimental static-thrust performance of rotor 2, H/D = 0.080 (ref. 3).....	4
5 Experimental results and equivalent solidity single rotor theory for level flight. $\sigma(\text{coaxial}) = 0.054$, $\sigma(\text{single}) = 0.027$, H/D = 0.093 (ref. 4).....	4
6 Schematic of the advancing blade concept (ref. 7).....	5
7 Comparison of theoretical and experimental static-thrust performance of model ABC rotor, H/D not reported (ref. 7).....	5
8 Effect of rotor separation on ABC performance prediction (ref. 8).....	6
9 Underestimation of ABC rotor inflow at low speed (ref. 11).....	7
10 Flight test rotor of merit for XH-59A in OGE hover (ref. 13).....	7
11 Induced power correction coefficient vs. blade linear twist for various taper ratio values (ref. 26).....	8
12 Coefficients k_T and k_{pr} vs. blade taper ratio (ref. 26).....	8
13 Comparison of single rotor theory (ref. 26) with experimental results (ref. 3) as reported in reference 31.....	8
14 Comparison of the coaxial with other helicopter types (ref. 31).....	10
15 Coaxial rotor in a wind tunnel (ref. 27).....	10
16 Areas of "unsteady flapping" motion for single and coaxial rotors (ref. 34).....	10
17 Ka-32 blade separation distance as a function of advance ratio (ref. 34).....	11
18 Calculated velocity field for the vortex ring condition, H/D = 0.10, $v = 0.2$ (ref. 28).....	11
19 Calculated velocity field for edgewise flow in longitudinal/vertical plane, H/D = 0.10, $\mu = 0.10$ (ref. 28).....	11
20 3/rev vertical vibration of the Ka-25 at the center of gravity (ref. 33).....	12
21 Coaxial rotor phasing: (a) ULYSS-6 solution, (b) flight test solution.....	12
22 3/rev vertical vibration of the Ka-50 at an unspecified location (ref. 33).....	12
23 Effective increase of coaxial rotor disc area (ref. 32).....	12
24 Experimental results for coaxial and equivalent solidity, single rotors in hover, D = 8.2 ft (2.5 m), H/D not reported (ref. 32).....	12
25 Comparison of overall helicopter efficiencies (ref. 32).....	13
26 National Defense Academy experimental apparatus (ref. 39).....	13
27 Tip vortices from both the upper and lower rotor were seen to have a faster axial speed when compared to Landgrebe's predictions, H/D = 0.105 (ref. 39).....	14
28 Effect of mutual interaction on rotor performance in hover, H/D = 0.132 (ref. 40).....	14
29 System hover performance, H/D = 0.132 (ref. 40).....	15

30	Effect of separation distance on the optimal performance of the hovering system (ref. 40).....	15
31	Wake model for a coaxial rotor in hover (refs. 41 and 43).....	15
32	Rotor mutual interaction factors, developed from references 41 and 43.....	16
33	Effect of axial spacing on optimum thrust and power ratios (refs. 41 and 43).....	17
34	Simplified sketches of typical flow visualization results (refs. 41 and 43).....	17
35	An example of computed wake geometry at $H/D = 0.10$ (refs. 41 and 43).....	17
36	Comparison of theoretical (ref. 42) and experimental (ref. 39) static-thrust performance, $H/D = 0.13$	18
37	Performance characteristics as a function of advance ratio, showing large influences of upper rotor on lower, $H/D = 0.316$ (ref. 38).....	18
38	Comparison of optimum pitch angle differences (ref. 38).....	18
39	Optimum coaxial vs. single rotor performances in hover and forward flight (ref. 38).....	19
40	Hover theory (ref. 45).....	19
41	Comparison of Landgrebe and coaxial rotor wake limits (ref. 44).....	20
42	Comparison of experimental and theoretical Mote forward flight performance (ref. 45).....	21
43	Comparison of experimental and theoretical Mote performance, $\mu = 0.174$ (ref. 45).....	21
44	Discontinuous theory vs. experimental results of references 3 and 46.....	21
45	Static-thrust prediction incorporating automatic contraction of tip vortices.....	22

Nomenclature

b	number of blades	z	vertical distance
C_Q	torque coefficient	α	contraction ratio of upper rotor wake at lower rotor
$(C_{Q_{pr}})_{co}$	coaxial rotor profile-drag torque coefficient	ϵ_1	thrust loss due to rotation of fluid in rotor wakes
C_T	thrust coefficient	ϵ_2	power loss due to rotation of fluid in rotor wakes
c	blade chord	η	overall helicopter efficiency
c_d	profile-drag coefficient	η^*	blade taper ratio = c_{root}/c_{tip}
c_{l_o}	average blade-lift coefficient	θ	rotor collective angle
D	rotor diameter	θ_{tw}	blade twist angle
FOM	rotor figure of merit	λ	nondimensional wake velocity
H	vertical rotor separation distance	μ	advance ratio = $V/\Omega R$
H/D	nondimensional rotor separation distance	v	descent ratio = $W/\Omega R$
I_o	induced power correction coefficient	v	power sharing ratio (figs. 33 and 35)
K_{Γ_i}	circulation of fluid at each station in wake	ξ_{py}	tail rotor loss coefficient
k, k', k''	axial velocity influence factors, functions of axial spacing	ξ_{Tp}	transmission efficiency coefficient
k_{pr}	influence of taper on torque coefficient	ρ	air density
k_T	influence of taper on thrust coefficient	σ	rotor solidity = $bc/\pi R$
\bar{P}	total induced power	τ	thrust sharing ratio between rotors = T_{low}/T_{upp}
Q	rotor torque	ϕ	inflow angle
R	rotor system radius	ψ	azimuthal position of rotor blade
$Re_{0.75}$	Reynolds number at 75% rotor radius	Ω	rotational speed of rotors
r	radial distance	ω	swirl velocity of fluid
T	rotor thrust	Subscripts	
\bar{T}	thrust/weight ratio	co	coaxial
V	forward velocity of helicopter	l, low	lower rotor
W	vertical descent velocity of helicopter	O	outer region of rotor or wake
w	axial velocity of fluid	u, upp	upper rotor

A Survey of Theoretical and Experimental Coaxial Rotor Aerodynamic Research

COLIN P. COLEMAN

Ames Research Center

Summary

The recent appearance of the Kamov Ka-50 helicopter and the application of coaxial rotors to unmanned aerial vehicles have renewed international interest in the coaxial rotor configuration. This report addresses the aerodynamic issues peculiar to coaxial rotors by surveying American, Russian, Japanese, British, and German research. (Herein, "coaxial rotors" refers to helicopter, not propeller, rotors. The intermeshing rotor system was not investigated.) Issues addressed are separation distance, load sharing between rotors, wake structure, solidity effects, swirl recovery, and the effects of having no tail rotor. A general summary of the coaxial rotor configuration explores the configuration's advantages and applications.

Introduction

In 1859, the British Patent Office awarded the first helicopter patent to Henry Bright for his coaxial design, as shown in figure 1 (ref. 1). From this point, coaxial helicopters developed into fully operational machines as we know them today. The Kamov Design Bureau has

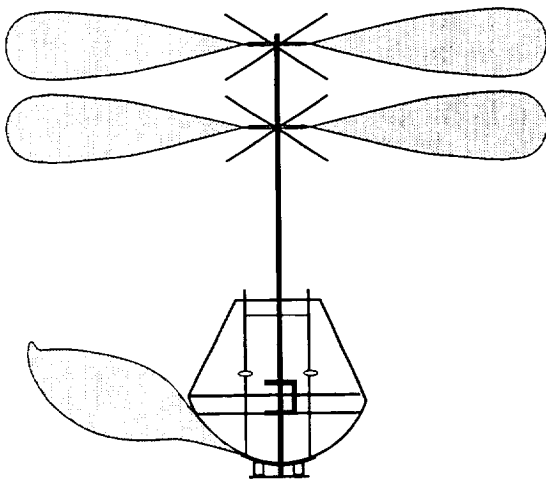


Figure 1. Henry Bright's 1859 coaxial design patent (ref. 1).

historically led the design and production of these designs for civilian applications and the Soviet Navy; moreover, the appearance of the Kamov Ka-50 helicopter proved that the coaxial rotor configuration could be applied to military attack helicopters. Western trends, however, have concentrated on single main rotor/tail rotor, tandem rotor, and synchropter devices. An exception to this is shipboard launched short-range unmanned aerial vehicles (UAV), such as the Israeli Hellstar, where the need for vertical takeoff and landing capability combined with stable handling characteristics has renewed interest in the coaxial configuration.

According to Lambermont (ref. 1), the Hiller Aircraft Company produced the first successful American coaxial helicopter in 1944. Hiller went on to produce the XH-44, which was followed by Bendix (Models K and J), Hoppicopter, Brantly, Roteron, and Jenson. When Bendix dissolved in 1949, they sold their Model K to the National Advisory Committee for Aeronautics (NACA) Langley Research Center for rotor research work and their Model J to the Gyrodyne Company of America. During the 1950s, NACA Langley used their rotor as part of a program to investigate the general characteristics of multiple-rotor configurations in the Langley full-scale tunnel, which was also supplemented by small-scale model tests (refs. 2-4). Gyrodyne continuously worked to improve the coaxial rotor helicopter concept over a number of years (ref. 5). After converting the Bendix Model J to the Model 2C, problems arose such as vertical rudders and differential collective failing to provide adequate yaw control in autorotation. March 1953 saw the idea of using "tip brakes," which solved this problem. Gyrodyne went on to develop the XRON and YRON series, followed by the QH-50 series, which served as a remotely controlled, weapon-carrying drone used for antisubmarine warfare. Over 700 QH-50s were subsequently built and delivered to the U.S. Navy. The Gyrodyne concept is currently being pursued under license by Dornier GmbH (Germany) and Israeli Aircraft Industries, Ltd. (Israel). The coaxial rotor concept was also pursued by Sikorsky Aircraft via the advancing blade concept (ABC) helicopter, which culminated in two flight vehicles (refs. 6-23).

Russia's first involvement in coaxial helicopters can be traced back to 1908–1910 when I. I. Sikorsky (then a student of the Kiev Polytechnical Institute) built two machines (ref. 24). The A. S. Yakovlev Aircraft Design Bureau built an experimental coaxial helicopter at the end of 1944. In 1945, N. I. Kamov formed his research group with the objective of building a small, single-seat coaxial helicopter called the Ka-8 (first flight in 1947). Through progressive incremental steps of experimentation and theoretical development, the Kamov Design Bureau, currently the world's largest producer of coaxial rotor helicopters, designed and produced a series of increasingly sophisticated coaxial helicopters (refs. 25–37).

The National Defense Academy in Yokosuka, Japan, conducted a program to study the aerodynamics of the coaxial rotor configuration in hover and forward flight during the late 1970s and early 1980s (refs. 38–43). Extensive experimental tests were conducted to understand the wake structure and its relationship to rotor performance as a function of collective, rotor spacing, and system thrust level.

Andrew (refs. 44 and 45) of the United Kingdom and Zimmer (ref. 46 and private correspondence, Jan. 25, 1993) of Germany both conducted investigations of the coaxial rotor configuration as a result of UAV activity. Andrew used a prototype UAV from Westland Helicopter Ltd. as his experimental test bed (ref. 47), while Zimmer's efforts have been related to Dornier's development of the QH-50 under license from Gyrodyne.

This report surveys coaxial rotor aerodynamic research during the past half century and concludes by summarizing the basic aerodynamic effects of rotor spacing, collective settings on both rotors (differential collective), thrust and torque sharing ratios between the rotors, wake structure and its difference from single rotors, mutual interaction effects, and optimal performance. Most of the surveyed papers are in the public domain. Soviet notation has been converted to American notation.

Definitions

- A coaxial rotor is defined as having an upper and a lower rotor that rotate in opposite directions to each other. Since torque balance is achieved with the main rotor system, a tail rotor is not required.
- The solidity of a coaxial rotor (σ) is defined the same way as for a single rotor:

$$\sigma = \frac{bc}{\pi R}$$

where b is the total number of blades, c is the blade chord, and R is the radius of the rotor system. (Note that the disc area used in the above expression is the disc area of just one of the two rotors, πR^2 .) Throughout this report, comparisons are often made with single rotors having the same solidity as a coaxial rotor. However, there will be occasions when a single rotor is used that has a solidity that is half that of the coaxial's.

- Given a rotor of diameter D and vertical rotor separation distance H , the nondimensional rotor separation distance is defined as H/D .
- The coaxial rotor figure of merit (FOM) has the same form as for a single rotor and is defined as:

$$\text{FOM} = \frac{C_{T_{\text{co}}}^{3/2}}{\sqrt{2}C_{Q_{\text{co}}}}$$

where

$$C_{T_{\text{co}}} = \frac{T_{\text{upp}} + T_{\text{low}}}{\rho(\Omega R)^2 \pi R^2} \quad (\text{thrust coefficient})$$

$$C_{Q_{\text{co}}} = \frac{Q_{\text{upp}} + Q_{\text{low}}}{\rho(\Omega R)^2 \pi R^3} \quad (\text{torque coefficient})$$

Research in the United States of America

NACA Langley Research Center

The aerodynamics of a 1.67 ft (0.509 m) diameter coaxial rotor in the static-thrust condition was investigated by Taylor (ref. 2) in 1950. The rotor had $H/D = 0.17$, solidity of 0.08, and $Re_{0.75} = 0.0825 \times 10^6$. Flow visualization was accomplished by introducing balsa dust into the air flow and photographing the results. For the coaxial configuration, it was found that the vortex filaments emanating from the blade tips of the upper and lower rotors did not merge or cancel one another but retained their separate identities in the wake. Taylor reported that "the blade-tip vortex patterns for the upper and lower rotors of the coaxial configuration bracket the pattern obtained for the single-rotor arrangement due to mutual interference effects." This implied that the upper and lower rotor wakes contracted radially inward at a faster and slower rate, respectively, than an isolated single (upper or lower) rotor and that this effect was caused by rotor mutual interaction.

An experimental investigation of the static-thrust performance of a coaxial rotor was carried out by Harrington in the Langley full-scale tunnel in 1951 (ref. 3). Two untwisted 25 ft (7.62 m) diameter rotors

Table 1. Testing conditions for Harrington's experiment (ref. 3)

	Configuration	σ	V_{tip} (ft/sec)	$Re_{0.75}$
Rotor 1	Single lower	0.027	500	1.3×10^6
	Single upper	0.027	500	1.3×10^6
	Coaxial	0.054	500	1.3×10^6
	Coaxial	0.054	450	1.1×10^6
	Coaxial	0.054	327	0.8×10^6
Rotor 2	Single lower	0.076	392	2.8×10^6
	Single lower	0.076	262	1.9×10^6
	Coaxial	0.152	392	2.8×10^6
	Coaxial	0.152	327	2.3×10^6

were tested in both coaxial and single-rotor configurations. Rotor 1 had $H/D = 0.093$ with blades tapered in planform and thickness. The maximum disc loading of rotor 1 was 3.3 lb/ft^2 (158 N/m^2). Rotor 2 had $H/D = 0.080$ with blades tapered in thickness but not in planform. The maximum disc loading for rotor 2 was 2.5 lb/ft^2 (120 N/m^2). Testing conditions are given in table 1.

When rotor 1 was tested, a performance offset caused by scale effect was observed at a tip speed of 327 ft/sec ($Re_{0.75} = 0.8 \times 10^6$), which led to an average 7% increase

in power for a given thrust (fig. 2). This scale effect was lessened for tip speeds of 450 and 500 ft/sec, ($Re_{0.75} = 1.1 \times 10^6$ and 1.3×10^6 , respectively). Differential collective pitch was also applied to both rotors to deliberately create a non-torque-balanced coaxial system. This resulted in a 2% increase in power compared with the torque-balanced data. Figure 3 summarizes Harrington's figure of merit results for rotor 1. The calculated difference is due to a difference in solidity (0.027 vs. 0.054) and not due to a difference in rotor configuration.

Both rotors 1 and 2 were compared with the equivalent solidity, single-rotor theory, and both show the same trend. Figure 4 shows the results of rotor 2 testing, together with theory comparison. The hovering theory did remarkably well in the prediction of the single rotor's hovering performance, and was only slightly in error for

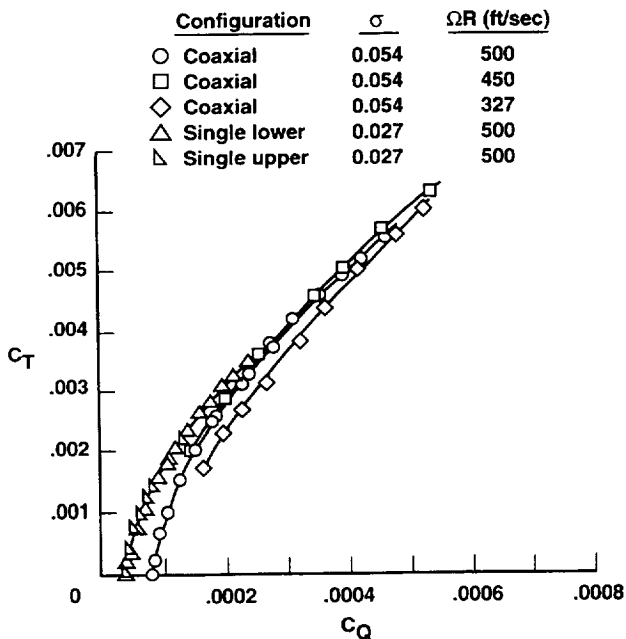


Figure 2. Scale effect on rotor 1 performance at 327 ft/sec, $H/D = 0.093$. Lines drawn through data (ref. 3).

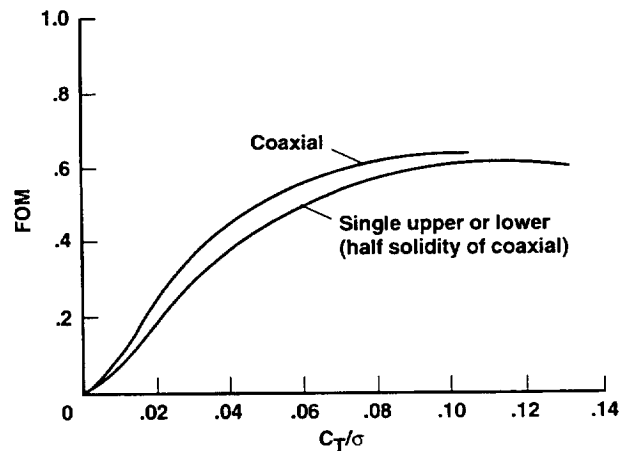


Figure 3. Effect of solidity on rotor figure of merit (ref. 3).

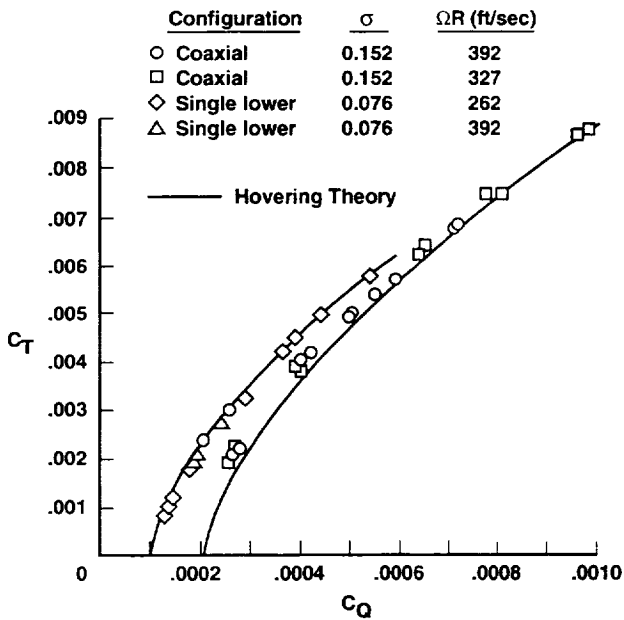


Figure 4. Comparison of theoretical (solid line) and experimental static-thrust performance of rotor 2, $H/D = 0.080$ (ref. 3).

the coaxial rotor for most of the thrust coefficients tested. On average, the theory predicted about 5% more power required for a given thrust than was shown in the experimental results, and this difference decreased to zero at the highest thrust coefficients tested. Because of the accuracy with which the theory predicted the two different single rotors, it was inferred that any difference between the coaxial experiment and single-rotor theory was the result of an aerodynamic anomaly that is not present in single rotors. However, Harrington did not state this, and it was generally accepted that the single-rotor theory was good enough for coaxial performance prediction.

The validity of the single-rotor theory was questioned by Dingledein (ref. 4); he proposed that the tips of the lower rotor would stall at high thrust coefficients and would therefore not be modeled. A recomparison of the equivalent single-rotor theory with experimental coaxial measurements (using rotor 1 from Harrington's experiments) showed the same results as above ($Re_{0.75} = 1.3 \times 10^6$). He concluded that the equivalent solidity, single-rotor theory was sufficient (within the bounds of experiment accuracy) to use as a performance prediction method for a coaxial rotor in hover.

The forward flight performances of single and coaxial rotors were also obtained by Dingledein (ref. 4) using rotor 1. The tests were performed at constant thrust coefficient and rotor speed for various advance ratios (fig. 5). The theoretical predictions for a single rotor

agreed well with the experimental single rotor. It was found that up to 14% more power was required for the coaxial rotor than for a theoretical single rotor of equivalent solidity under the same conditions. It was concluded that this difference was caused by increases in both profile and induced losses associated with interference effects. Analysis methods employed at that time (ref. 48) could not model this effect. Dingledein concluded, "the indications remain, however, that the coaxial arrangement tested required more power in forward flight than an equivalent single rotor, although there are certain advantages to the configuration which may offset the larger power requirement in certain applications."

De Lackner Helicopters, Inc.

Development problems with the De Lackner DH-4 Aerocycle in the late 1950s led to a flight demonstration accident at about 16 knots. Speculative reasons for the accident included the coaxial rotors striking each other (because of blade bending) and uncontrollable longitudinal oscillations. In 1959, the Aerocycle was tested in the Langley full-scale wind tunnel (ref. 49). The objectives of this test were to measure forces, moments, and static stability derivatives to find a probable cause for the crash, and to compare theory with experimental results. It was found that the forward speed was limited by an uncontrollable pitching moment, and that the tip clearance between the rotors was always sufficient. The blade-element/momentum-based theory of the isolated

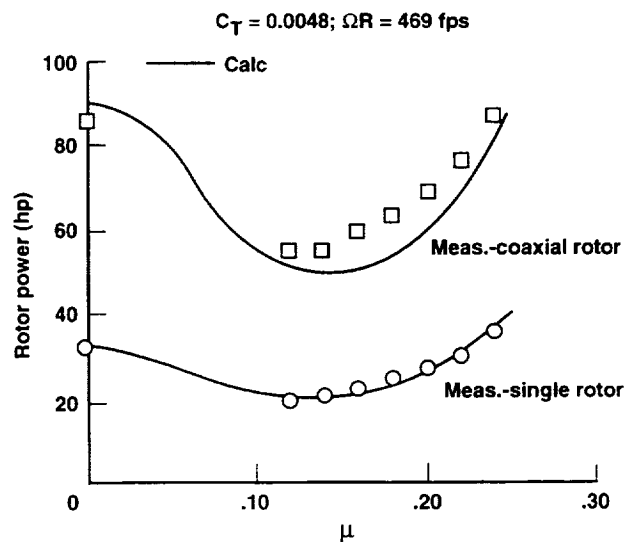


Figure 5. Experimental results and equivalent solidity single rotor theory for level flight. $\sigma(\text{coaxial}) = 0.054$, $\sigma(\text{single}) = 0.027$, $H/D = 0.093$ (ref. 4).

rotor system showed that “rigid-rotor pitching moments and static-stability derivatives may be predicted with reasonable accuracy, provided that a longitudinal inflow variation is assumed. Omission of the longitudinal inflow variation in some cases leads to large errors.”

Sikorsky Aircraft

The ABC rotor system, consisting of two coaxial counterrotating hingeless rotors with a small rotor spacing, took advantage of the aerodynamic lift potential of the advancing blades. At high speeds, the retreating blades were unloaded, with most of the load being carried on the advancing sides of both rotors, thereby eliminating the penalties of retreating blade stall (fig. 6).

Developmental work began in 1965 at the United Aircraft Research Laboratories (UARL) which included small-scale rotor tests and theoretical studies. Reference 7 summarizes this preliminary research, including several experiments using a 4 ft (1.22 m) diameter rotor. Hover testing (ref. 6) was carried out during which collective, rotor spacing, and inter-rotor phase angle were altered. Performance data and flow visualization pictures were taken in order to compare coaxial with single rotors. Vortices from the upper rotor were seen to move radially inward and downward faster than vortices from the lower

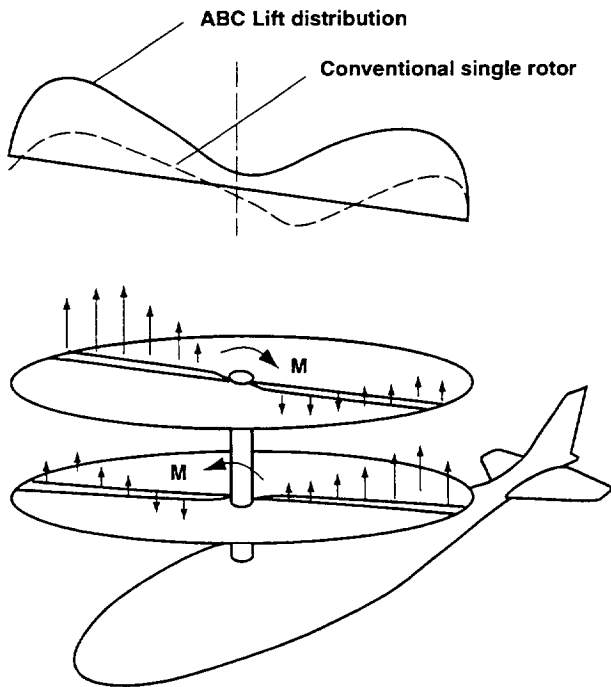


Figure 6. Schematic of the advancing blade concept (ref. 7).

rotor. Figure 7 shows performance data at an unspecified rotor spacing. Total power for the coaxial rotor experiment was 3–9% less than the equivalent single-rotor theory; these results are comparable to those obtained by Harrington (ref. 3). It was inferred that there was a beneficial effect on total performance which was attributed to reduced swirl velocity in the rotor wake, although this conclusion can not be justified based on the experimental results. It was also concluded that rotor spacing had little effect on performance (although only two different rotor spacings were tested). Forward flight performance and blade stress characteristics were examined with a 1/10-scale rotor with dynamically scaled blades. Forward speeds from 60 to 180 knots were tested, with spacings between $H/D = 0.07$ and $H/D = 0.10$; no significant effects on performance or stress were observed.

The prototype XH-59A was designed for 14,500 lb (64,500 N) gross weight, maximum forward speed of 230 knots using a 40 ft (12.19 m) diameter rotor with -10° nonlinear twist. Development of the rotor was reported in reference 9.

The XH-59A rotor was tested in the NASA Ames 40-by 80-Foot Wind Tunnel and reported in 1971 (refs. 8 and 9). Advance ratios tested were from 0.21 to 0.91. Reference 8 includes the theoretical modeling of the rotor, in which the top rotor has a uniform induced velocity based on one-half of the system’s lift, while the

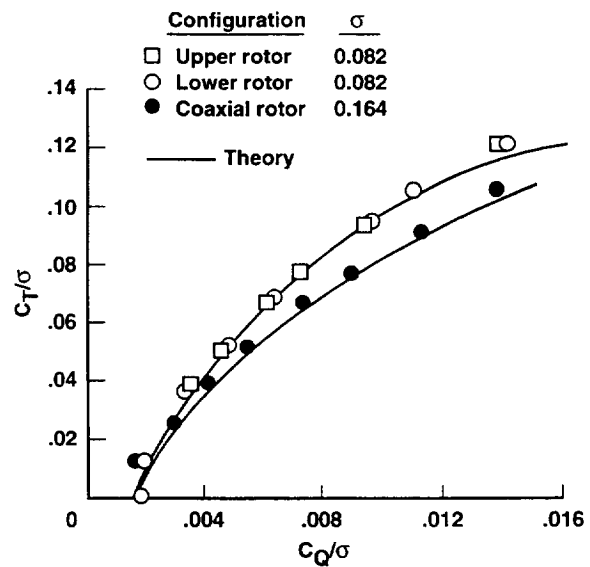


Figure 7. Comparison of theoretical and experimental static-thrust performance of model ABC rotor, H/D not reported (ref. 7).

lower rotor experiences the sum of the upper rotor's induced velocity (undeveloped wake) plus its own induced velocity. No differential pitch was used to compensate for the difference in yawing moments between the two rotors. Figure 8 (from ref. 8) compares the "dual rotor theory with wake interference" with rotor measurements. Dual rotor theory was shown to be an improvement over the single-rotor theory, especially at low advance ratios, where one would expect the influence of the upper rotor to be the greatest. No significant differences were seen in the prediction of drag for the rotor system. Reference 8 concluded that "the comparison of single and dual rotor torque, as predicted by the methods herein, indicates a performance benefit (torque reduction) for the dual rotor over that of a single rotor of equivalent disc loading. Thus, it appears that the performance benefits obtained by operating the upper rotor in a more favorable velocity field are more significant than the performance decrement caused by operating the lower rotor in the downwash of the upper rotor." Comparing figure 8 with figure 5, we see that this result is in disagreement with Dingledein's result (ref. 4). Wake interference effects were also examined using two different wake models. The first model included a wake in which the lower rotor was subjected to a noncontracting upper rotor wake. The second model included a wake in which the lower rotor was subjected to a fully developed upper rotor wake over the inboard 50% of the rotor, thus simulating a high degree of wake contraction and acceleration. Predicted torque associated with this second method of calculation was reduced, indicating that greater performance efficiency could be obtained when outboard sections of the lower rotor escape upper rotor downwash. Reference 8 also concluded that "single rotor theory may be used as a simple method of calculating coaxial rotor performance so long as inflow variations, differential control inputs, and blade geometry differences are considered second order effects."

In 1973, a 1/5 Froude scale model ABC was tested at the Princeton University Dynamic Model Track (ref. 10). The test examined the low-speed dynamics and aerodynamics of the ABC coaxial rotor helicopter (from hover to $\mu = 0.1$). This range was of particular interest because rotor-induced velocity was large relative to forward speed so that mutual interference effects on the airframe were substantial. Static and dynamic tests were carried out, as well as a vibration evaluation. The tests confirmed the high level of cyclic control power predicted by theory and showed that selection of the proper control system phasing permitted trimming of the ABC from hover through transition. No significant vibration problems were encountered at low advance ratio.

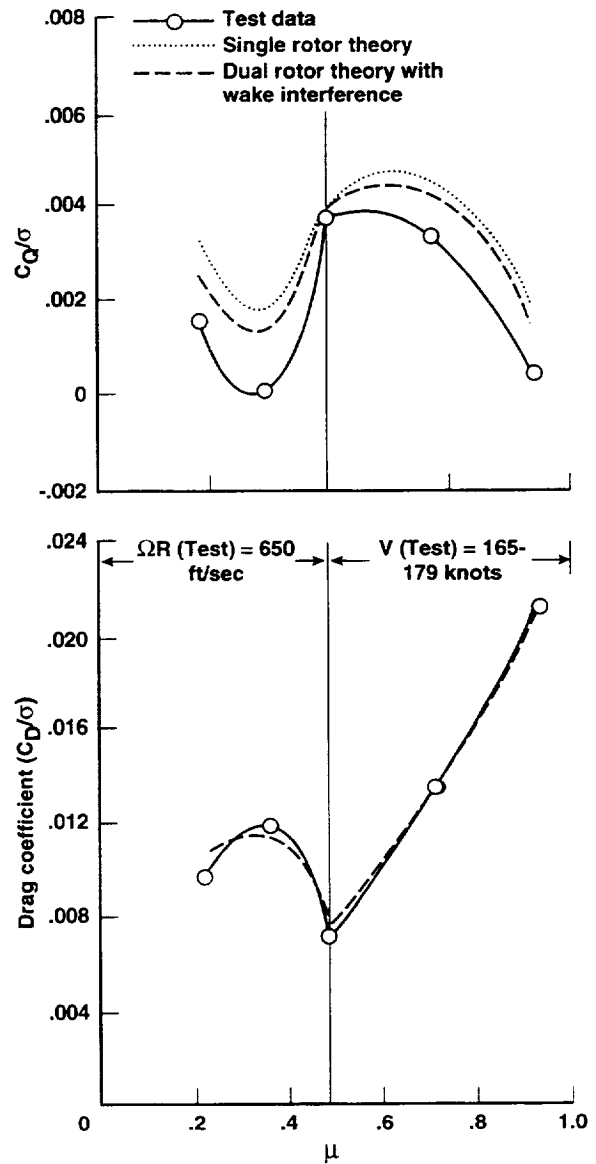


Figure 8. Effect of rotor separation on ABC performance prediction (ref. 8).

The first flight of the ABC aircraft (XH-59A) in pure helicopter mode occurred July 26, 1973. The aircraft had a 36 ft (10.97 m) diameter rotor, $H/D = 0.069$, total rotor solidity of 0.127, blade taper ratio of 2:1 with -10° nonlinear twist, and disc loading of 10.3 lb/ft^2 (493 N/m^2). On August 24, 1973, this first aircraft, while flying at 25–30 knots at an altitude of about 50 ft (15.24 m), pitched nose-up, lost altitude, and was extensively damaged in a hard, tail-first landing. A detailed accident investigation was subsequently conducted, involving wind tunnel tests of a 1/5 Froude scale model XH-59A aircraft. Results, projected to the full-scale XH-59A aircraft, disclosed a significant

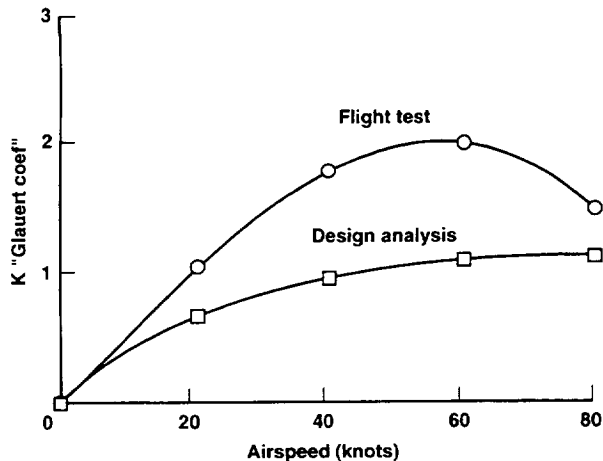


Figure 9. Underestimation of ABC rotor inflow at low speed (ref. 11).

difference between the analytically assumed fore-and-aft variation of inflow through the rotors and the actual inflow. The empirical "Glauert term" used to define this effect ($\cos \psi$ variation) significantly underestimated the actual conditions (fig. 9, ref. 11). Consequently, more forward longitudinal cyclic pitch was required for a given (low-speed) trim condition than had been predicted. Unfortunately, the forward longitudinal cyclic stick travel was deliberately rigged to prevent pilot overcontrol of the aircraft. The flight control system was then modified in the second test aircraft to essentially double the longitudinal and lateral cyclic control ranges. The first flight with this modified flight control system occurred in July 1975.

Continued expansion of the flight envelope was reported in references 12–16. Reference 13 reported on an XH-59A flight test during which the aircraft was tethered to the ground. Hover performance both in and out of ground effect (OGE) was obtained in terms of power and gross weight coefficients. In calculating the rotor performance, it was assumed that the download on the fuselage was 6% of the rotor thrust, and that transmission and accessory losses resulted in a 95% transmission efficiency. From these assumptions, a plot of OGE rotor figure of merit versus C_T/σ was obtained (fig. 10). However, because of these loss estimates, the accuracy of these rotor performance results is questionable.

Sudden lateral accelerations in ground effect were also experienced during these flight tests (ref. 20) which were attributed to a Karman vortex street shedding from the cylindrical fuselage. This was counteracted by adding small strip spoilers along the fuselage.

Following completion of flight tests in the pure helicopter mode, two turbojet engines were added for auxiliary

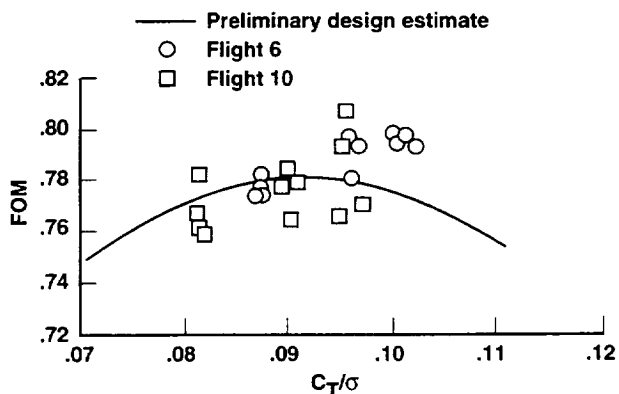


Figure 10. Flight test rotor figure of merit for XH-59A in OGE hover (ref. 13).

forward thrust in a high-speed configuration, and results from these flights are reported in references 19–21 and 23. In support of this, the 1/5 Froude scale model was tested at NASA Langley to evaluate the complete auxiliary propulsion speed envelope up to the 325 knot dive speed (ref. 17).

In 1980, the ABC was tested in the Ames 40- by 80-Foot Wind Tunnel to evaluate a rotor head drag reduction fairing and rotor/tail/propulsion system interference alleviation (ref. 22). Tests were conducted for advance ratios from 0.25 to 0.45 with the rotor on, and for free-stream velocities from 60 to 180 knots.

The ABC was never placed into production.

Research in Russia

Russia is the world's largest user of coaxial rotor helicopters. Their knowledge of the design can be attributed to both the work done by the Kamov Design Bureau and the research conducted by the Central Aerohydrodynamics Institute (TsAGI). Despite the extensive Soviet research, very few Soviet works have been translated and published in the West; only recently has some of this material been released. This section, therefore, summarizes only the reports that are currently available in this area (refs. 24–37).

Coaxial rotor aerodynamic theory is mentioned in two translated Soviet texts published in the West, "Theory of the Lifting Airscrew" (ref. 25) and "Helicopters" (ref. 26). The first of these covers a wide spectrum of analytical methods which include modeling blades by both lifting line and vorticity surfaces, using various wake types (free wakes and cylindrical wakes with skew angles from 0°

to 90°), and applying vortex (Joukowski) theory. These methods are simplified in "Helicopters" with an emphasis on obtaining practical application tools. Rotor blades are modeled solely by single lifting lines, and rotor wakes are assumed to be cylindrical in both hover and climb and flat in forward flight.

"Helicopters" proposes that the overall aerodynamic characteristics for the coaxial rotor can be found by treating it as an equivalent solidity, single rotor. This results in:

$$C_{Q_{co}} = (C_{Q_{pr}})_{co} + 0.79C_{T_{co}}^{3/2}I_o$$

where $(C_{Q_{pr}})_{co}$ is the coaxial rotor profile-drag torque coefficient, and I_o is an induced power correction coefficient, which reflects nonuniformity of the downwash (fig. 11). Assuming that the blades are tapered, the coaxial rotor profile torque coefficient is given as:

$$(C_{Q_{pr}})_{co} = \frac{1}{4}k_{pr}\sigma c_{d_o}$$

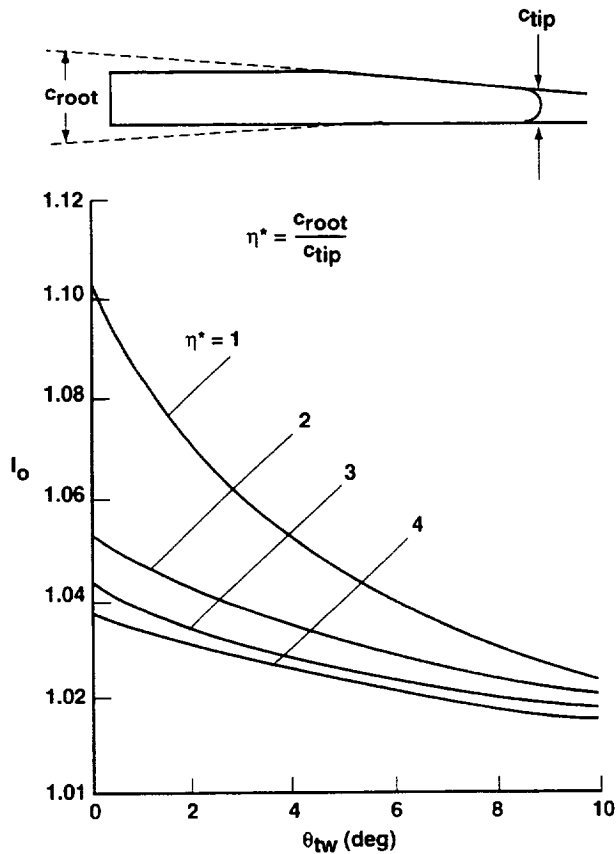


Figure 11. Induced power correction coefficient vs. blade linear twist for various taper ratio values (ref. 26).

where k_{pr} is a taper ratio influence coefficient (fig. 12), σ is the solidity of one of the two rotors making up the coaxial system, and c_{d_o} is the profile-drag coefficient at zero lift. For tapered blades, the thrust coefficient is given as:

$$C_{T_{co}} = 0.313k_T\sigma c_{l_o}$$

where the k_T coefficient reflects taper influence (fig. 12), and c_{l_o} is the average blade-lift coefficient.

These performance predictions were compared against Harrington's experiments (ref. 3) by Stepniewski et al. in figure 13 (ref. 31). Very similar results were achieved, and Stepniewski concluded that "'Helicopters' appears to be sufficiently accurate for preliminary performance estimates of coaxial rotors, assuming that the rotor tip speeds are not so high as to generate considerable compressibility effects outboard of the 0.7 blade station."

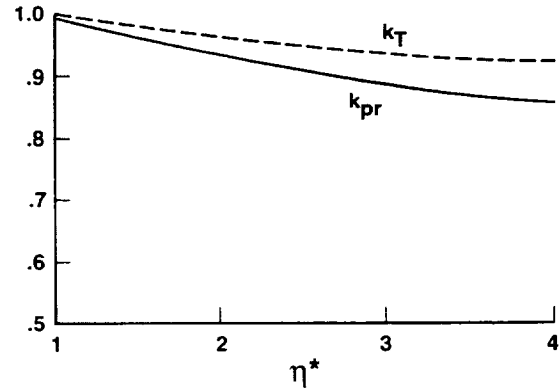


Figure 12. Coefficients k_T and k_{pr} vs. blade taper ratio (ref. 26).

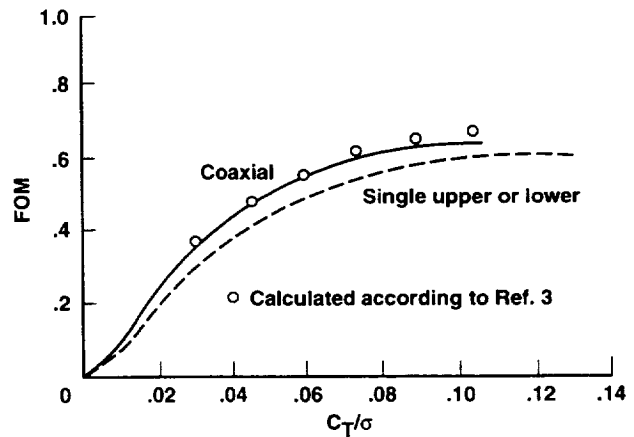


Figure 13. Comparison of single rotor theory (ref. 26) with experimental results (ref. 3) as reported in reference 31.

“Helicopters” (ref. 26) also develops a rotor performance estimate based on a separation distance of $H/D = 0.1$, which is a typical value. The individual rotors were treated as being in a climb, where the climb speed was equal to the velocity induced by the other rotor (and therefore different for each rotor). Solving for the induced velocities, it was found that $C_{T_{low}}/C_{T_{upp}} = 0.86$. Experiments by A. D. Levin (reported in ref. 26) on a coaxial rotor model of diameter 6.67 ft (2.034 m), $\sigma = 0.0445$, $H/D = 0.0985$ with blades of -12° twist and $C_{T_{co}} = 0.0036$ gave $C_{T_{low}}/C_{T_{upp}} = 0.87$. The main conclusion derived here was that “the average aerodynamic characteristics of a coaxial configuration are practically independent of the distance between the rotors.” According to reference 26, this conclusion is said to be confirmed by tests performed by Lessley reported in TsAGI Report No. 31, 1941, by V. I. Shaydakov who applied momentum theory (unreferenced) and also by V. S. Vozhdayev who applied blade vortex theory (unreferenced). It was also concluded that the “distance between rotors in the coaxial configuration affects only the distribution of thrust between the upper and lower rotors.” Consequently, a coaxial rotor in axial flight is treated as an equivalent solidity, single rotor, while accounting for the rotor mutual influence.

Forward flight phenomena in “Helicopters” were interpreted with the help of the flat-wake concept. Stepniewski (ref. 31) points out that this approach is strictly limited to advance ratios in the range $1.63 \sqrt{C_T} \leq \mu \leq 0.25$. If a flat wake is used (with the rotors generating the same torque), then it is assumed that the thrusts must also be equal, since each rotor will have an equal influence on the other. Experiments by A. D. Levin (reported in ref. 26) using the same apparatus as above found that for $\mu \geq 0.15$ and equal torques $C_{T_{upp}} = 1.05 C_{T_{low}}$. By measuring induced velocities, Levin also found that increasing the separation distance significantly reduced the influence of the mutually induced velocities. For $H/D = 0.0985$, he stated that “the induced power losses of the coaxial lifting system will be 21% lower than for a single rotor of the same diameter and doubled solidity.” He did not comment on the coaxial rotor’s parasite drag, nor on his method for finding the induced power. Based on “Helicopters” approximations, Stepniewski (ref. 31) compared the coaxial rotor with other helicopter configurations in forward flight (fig. 14). He concluded that “from the power required per unit of gross weight point of view, the classical coaxial helicopter with articulated rotors represents a configuration which, in spite of higher parasite drag than that of corresponding single-rotor or tandem machines, shows

an advantage in the engine power required in hover as well as at low and medium flying speed ranges.”

Another design method for coaxial rotors in axial flow was reported by Kvokov (ref. 36). The rotors were represented by lifting discs in which the circulation distribution was constant in azimuth but varied with radial position. A prescribed trajectory prepositioned the wake vortices. Assuming an ideal, incompressible fluid, expressions were obtained for the total induced velocity at an arbitrary point in the flow. Two-dimensional blade-element theory was used to calculate the lift and drag of the rotors, with profile-drag losses and a tip loss factor being added. The single-rotor wake geometry was also corrected to allow for the mutual interaction of the rotors (this was done by trial and error in matching experimental results obtained at TsAGI, and are unreferenced). Consequently, theoretical results were “tuned” to fit the experimental data.

A coaxial rotor experiment was described by Antropov (ref. 27). Figure 15 shows a rotor of 6.56 ft (2 m) diameter rotor with variable spacing ($0.06 < H/D < 0.12$) used for axial flight testing. The rotor system can also be tilted 90° into a vertical position, with the free-stream flow approaching edgewise, to simulate forward flight. Results of tests conducted by A. D. Levin (reported in ref. 27) using the above apparatus at $H/D = 0.088$ showed that the effect of the upper rotor on the lower is much greater than the reverse, and that this difference decreases with increasing advance ratio. The upper rotor was said to have the largest effect on the lower rotor at an advance ratio of 0.05, while the lower effects the upper the greatest at an advance ratio of 0.1 (no explanation given).

The aerodynamic coupling between the two rotors is strongly influenced by descending flight (ref. 34). Extensive experimental and theoretical research was carried out in the area of unsteady blade flapping motion (this phenomenon was not exactly defined). Figure 16 shows that this “unsteady flapping” motion is small when compared to a single rotor for various forward and vertical flight speeds. If such a reduction is possible, then the coaxial rotor configuration may possess blade vortex interaction characteristics different from those of the single-rotor helicopters in this condition. The minimum separation distance between any two passing blades as a function of advance ratio was also discussed by Anikin. Figure 17 shows the blade separation for the Ka-32 (presumably from flight test). At low advance ratios, the minimum distance occurs around $\psi = 270^\circ$ (ψ_5), and around $\psi = 90^\circ$ at higher speeds (ψ_2).

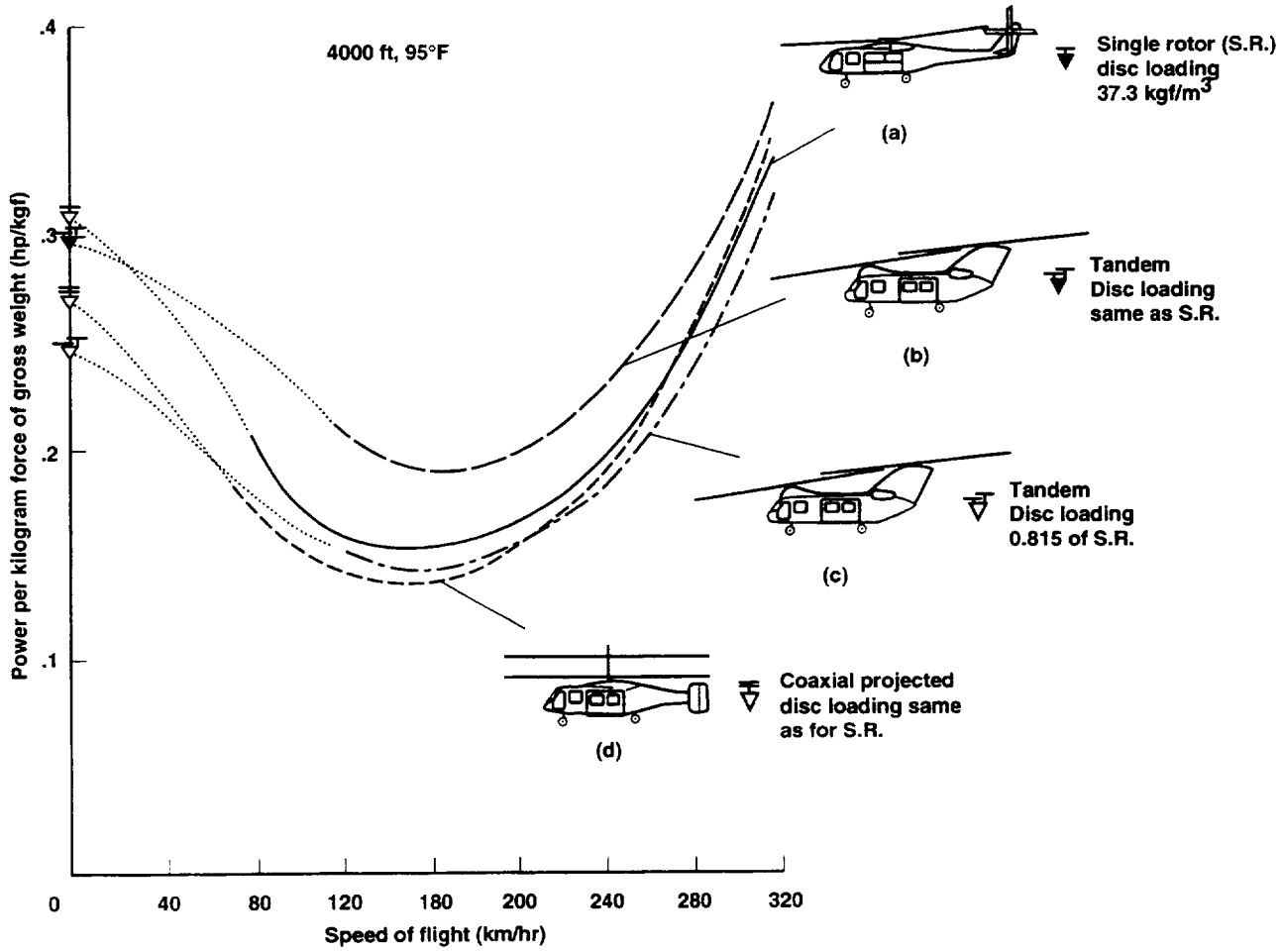


Figure 14. Comparison of the coaxial with other helicopter types (ref. 31).

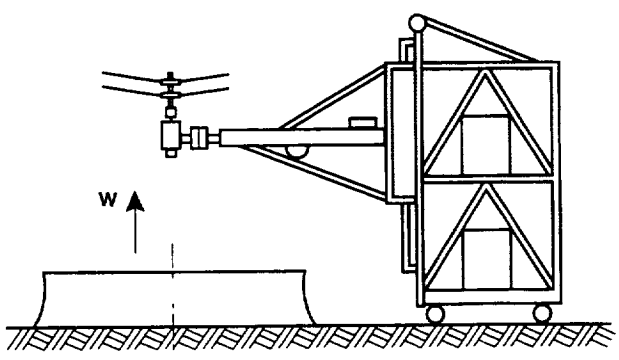


Figure 15. Coaxial rotor in a wind tunnel (ref. 27).

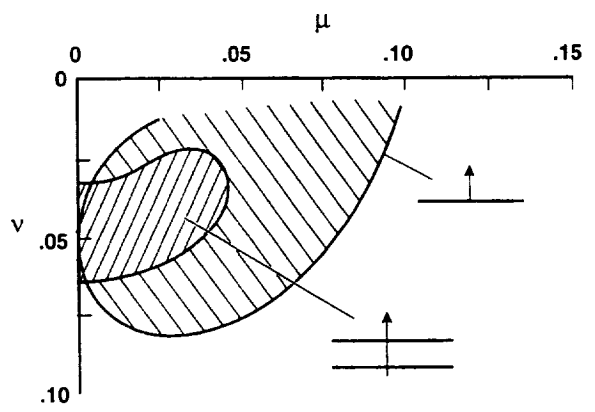


Figure 16. Areas of "unsteady flapping" motion for single and coaxial rotors (ref. 34).

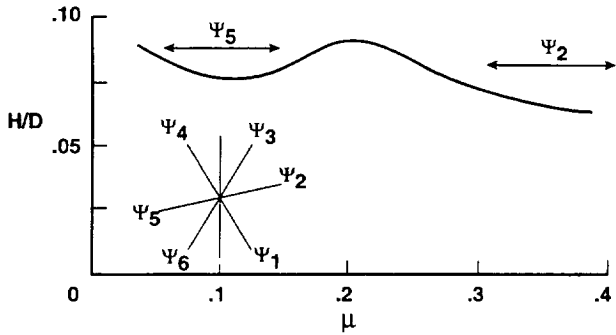


Figure 17. Ka-32 blade separation distance as a function of advance ratio (ref. 34).

A nonlinear vortex simulation of unsteady flow about a coaxial rotor in axial and edgewise flow was reported by Belotserkovskiy et al. (ref. 28). For coaxial rotors ($H/D = 0.1$) in axial descent, the vortex ring condition was found to occur at $v = 0.2$; figure 18 shows the velocity distribution at the tips of the rotors for this condition.

The decrease in thrust was explained by the existence of circulatory flow around the edge of the discs. Overall, the pattern is quite similar to a single rotor, although the cross

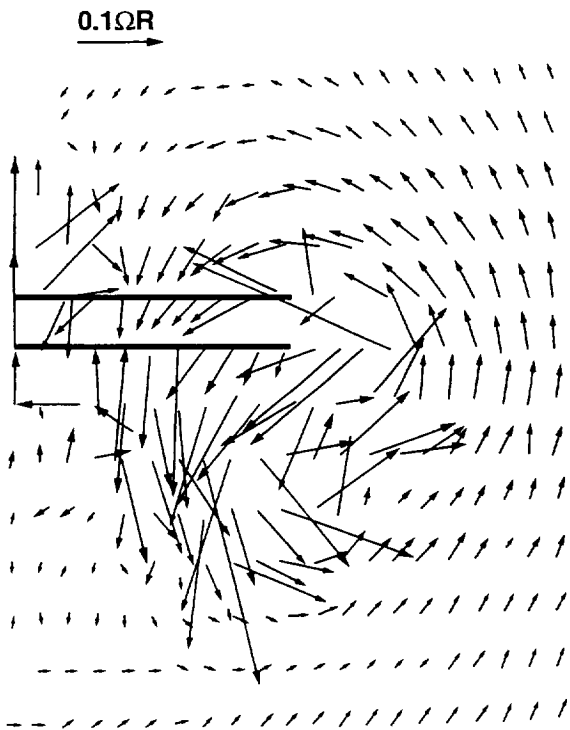


Figure 18. Calculated velocity field for the vortex ring condition, $H/D = 0.10$, $v = 0.2$ (ref. 28).

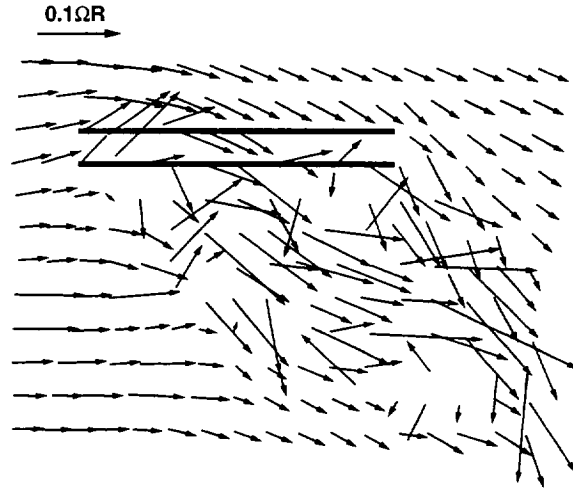


Figure 19. Calculated velocity field for edgewise flow in longitudinal/vertical plane, $H/D = 0.10$, $\mu = 0.10$ (ref. 28).

section of the vortex ring is more oblong and has an elliptical shape. Edgewise flight was computed for the same separation distance at an advance ratio of 0.1; figure 19 shows the wake for this case. Pronounced nonuniform induced velocities were found over the discs of the upper and lower rotors, and a "spillover" of the flow from the lower to upper rotor at the front of the discs was also calculated.

A lot of research has also gone into the aerodynamics of the coaxial rotor helicopter airframe, the most difficult part of which has been the empennage, which is in the aerodynamic shadow of the fuselage body (ref. 34). Usually two fins are fixed on the tips of a stabilizer connected to the fuselage at 65% rotor radius. The vertical and horizontal surfaces have to be larger than for a single rotor because of their small moment arms and the rapid deceleration of the airflow behind the poorly streamlined fuselage (these extra control surfaces lead to a higher drag penalty).

A vibration reduction program for coaxial helicopters was started in 1968 to see if the vertical vibration level could be reduced by altering the phase angle of the blade passage (ref. 37). Tests conducted on a Ka-25 showed that the 3/rev vertical vibration was reduced by arranging the blades to pass 15° off the longitudinal axis (as shown in fig. 21(b)), with this decrease being most apparent at the higher speeds (fig. 20). Burtsev (ref. 33) discussed a mathematical model developed by the Kamov Design Bureau called ULYSS-6, which was used to calculate this problem (ref. 37). Figure 21 shows that ULYSS-6 predicted a phase angle which was twice that observed in tests (no explanation given). Figure 22 shows the vertical vibration of the Ka-50 obtained from flight tests

(location of measurement not reported). From the similarity of this plot to that from the Ka-25 flight tests, it is assumed that the Kamov Design Bureau used a 15° phase angle for the Ka-50. This decrease in vertical vibration with speed is accomplished at the expense of the lateral vibration, which is deemed to be not so critical (ref. 37).

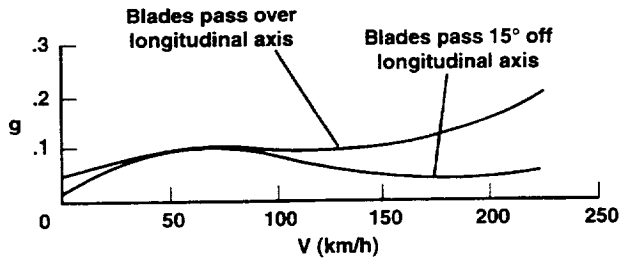


Figure 20. 3/rev vertical vibration of the Ka-25 at the center of gravity (ref. 37).

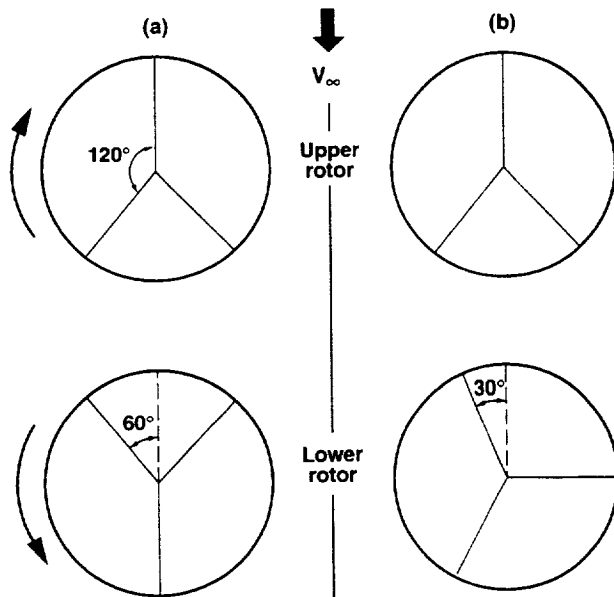


Figure 21. Coaxial rotor phasing; (a) ULYSS-6 solution, (b) flight test solution (ref. 37).

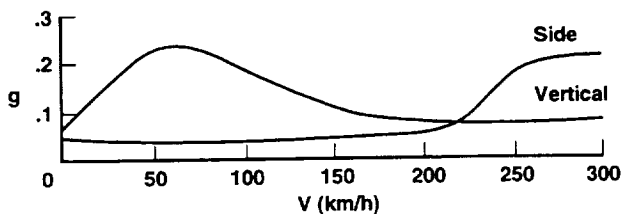


Figure 22. 3/rev vertical vibration of the Ka-50 at an unspecified location (ref. 37).

Soviet coaxial helicopter development as viewed from Russia was summarized by Kasjanikov in 1990 (ref. 32). He stated that coaxial features include a higher hovering efficiency compared to a single rotor, absence of a tail rotor, aerodynamic symmetry, and large deflections of longitudinal and lateral control forces. High hover efficiency is attributed to the mutual interference effects of the rotors, an effective increase of the disc area caused by extra clean air being drawn in by the lower rotor (fig. 23), and a reduction of the swirl in the wake. Experimental results obtained at TsAGI (unreferenced) showed that the rotor figure of merit for the coaxial rotor is much higher than for the single rotor of equal solidity (fig. 24),

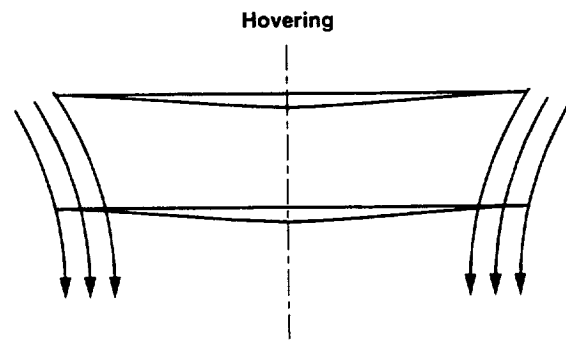


Figure 23. Effective increase of coaxial rotor disc area (ref. 32).

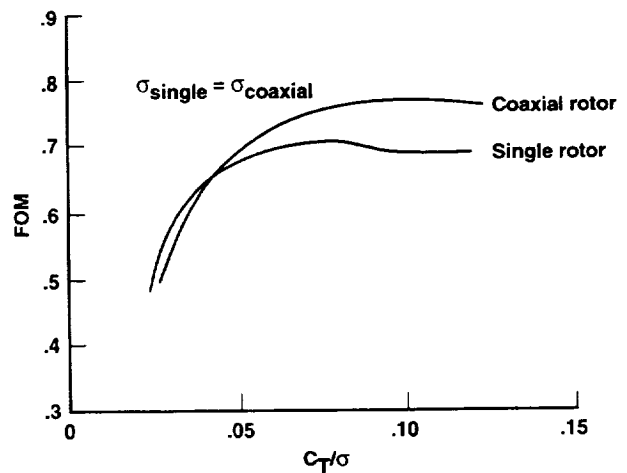


Figure 24. Experimental results for coaxial and equivalent solidity, single rotors in hover, $D = 8.2 \text{ ft (2.5 m)}$, H/D not reported (ref. 32).

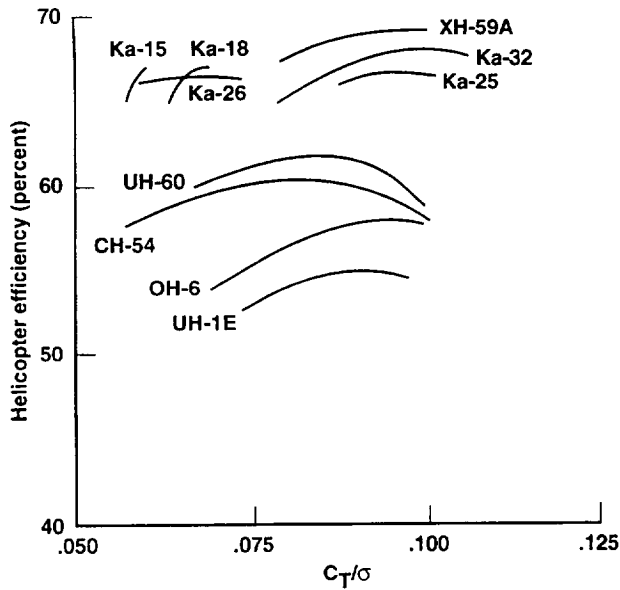


Figure 25. Comparison of overall helicopter efficiencies (ref. 32).

although these results appear to be significantly higher than those obtained by NACA and UARL. Helicopter efficiency (as a whole) was defined as:

$$\eta = \frac{\text{FOM} \xi_{T_p} \xi_{py}}{\bar{T}^{3/2}}$$

where ξ_{T_p} is the transmission efficiency coefficient, ξ_{py} is the tail rotor loss coefficient, and \bar{T} is the thrust/weight ratio. Using this definition, several helicopter efficiencies were compared in figure 25. Based on the above definition, Kamov estimated that the coaxial rotor helicopter has an overall efficiency 17–30% higher than for single-rotor helicopters.

Research in Japan

Experimental and theoretical research of the coaxial rotor configuration was carried out by Nagashima and others during the late 1970s and early 1980s (refs. 38–43). The basis for this work lay in treating the coaxial rotor as a type of variable geometry rotor (ref. 50). It was proposed that the coaxial rotor wake could be optimized with an appropriate selection of rotor parameters, which would lead to an improvement in performance compared to an equivalent single rotor. Experimental research utilized the apparatus shown in figure 26. The rotor had a diameter of 2.49 ft (0.76 m), $\sigma = 0.20$ with rotor spacing in the range $H/D = 0.105$ to 0.987. The rotor blades were untwisted, of rectangular planform, with a NACA 0012 section and a

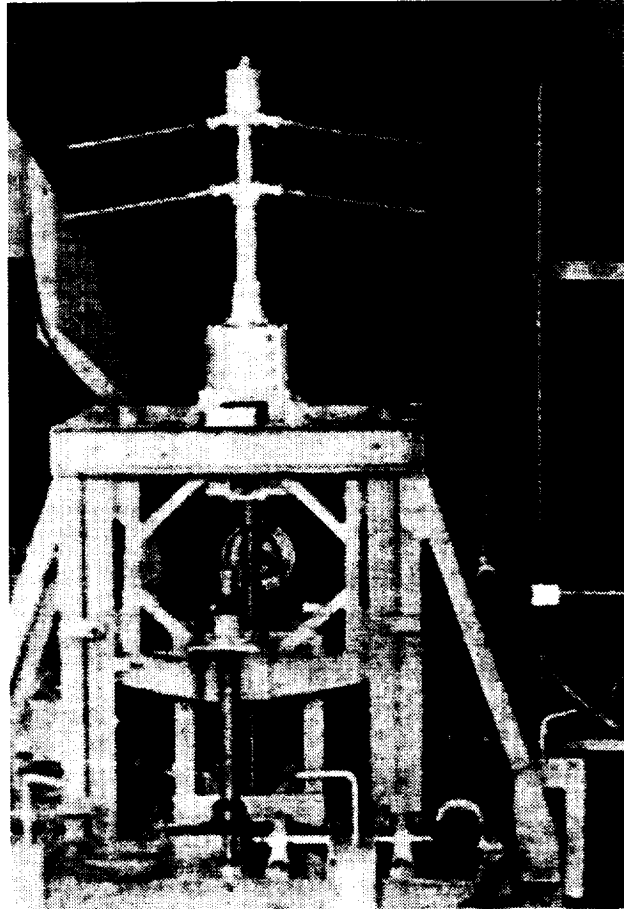


Figure 26. National Defense Academy experimental apparatus (ref. 39).

blade chord of 0.197 ft (0.60 m). The rotor speed was 3100 rpm, giving $Re_{0.75} = 0.38 \times 10^6$. (This Reynolds number is well below the value of 0.8×10^6 , which was shown by Harrington (ref. 3) to have a performance offset caused by scale effect.) Maximum disc loading for the system was approximately 5.5 lb/ft² (263 N/m²). A mixture of heated liquid paraffin and pressurized carbon dioxide was injected into the flow near the tips of the rotors to visualize the tip vortices.

Hover

A flow visualization study of the tip vortex geometry of the above model coaxial rotor in hover was reported by Nagashima et al. (ref. 39). A single four-bladed rotor was first run in isolation at three different pitch settings, and its tip vortex trajectories were found to be in good agreement with the prescribed values of Landgrebe (ref. 51). The coaxial rotor was then tested at the same

thrust level for three different spacings. The tip vortices from both the upper and lower rotors were seen to have a faster axial speed when compared to Landgrebe's predictions (fig. 27). The lower rotor wake was also seen to have a slower radial velocity, and so appeared to be "pushed out" farther than Landgrebe's wake (the upper rotor radial wake position being very close to predictions). These observations support those of Taylor (ref. 2) and UARL (ref. 6). In general, the rotor with the highest collective setting dominated the flow field around the system (ref. 40). However, when the lower rotor collective was 1° higher than the upper rotor ($\theta_{low} = \theta_{upp} + 1^\circ$), a different flow field was observed in which neither rotor dominated. The tip vortices from both rotors were equally spaced in the wake and moved at higher convection speeds than for a single rotor. This was particularly striking, since this differential collective setting was almost equal to that obtained for optimum performance from the force balance results. It was not clear from the flow visualization photographs what effect rotor spacing had on obtaining optimum performance. It was inferred that the faster axial convection speed of the tip vortices, together with the tip vortices being more evenly spaced, led to an increased performance of the coaxial versus the equivalent solidity, single rotor (as reported in ref. 40).

Experimentally obtained performance data were presented by Nagashima et al., in reference 40. Figure 28 shows the effect of mutual interaction on rotor performance in hover. As one would expect, the upper rotor has a big

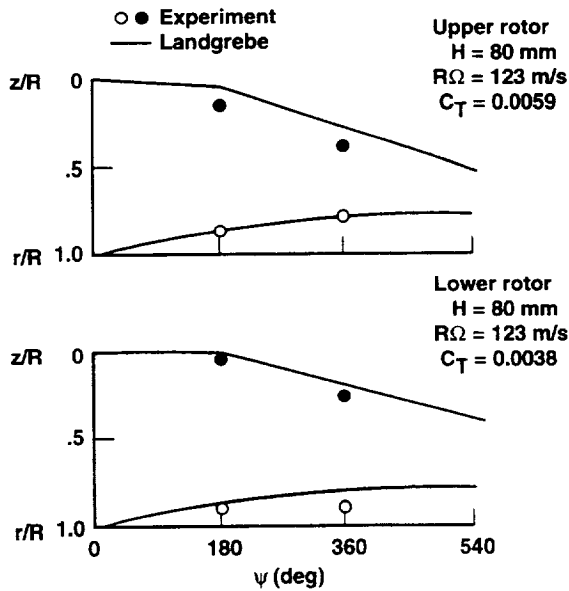


Figure 27. Tip vortices from both the upper and lower rotor were seen to have a faster axial speed when compared to Landgrebe's predictions, $H/D = 0.105$ (ref. 39).

influence on the performance of the lower rotor, as shown by the curves labeled (b). Perhaps surprising is the extent to which the lower rotor influences the upper rotor performance (curves labeled (a)). Note that most of these points are for non-torque-balanced cases. The hover performance of the system was then obtained as the algebraic sum of these two curves (fig. 29). Defining the "optimum pitch angle combination" to be the pair of pitch angles that maximizes C_T/C_Q for a given thrust, they determined that $\theta_{low} = \theta_{upp} + 1.3^\circ$ gave the best performance for $H/D = 0.105$ (and $\theta_l = \theta_u + 1.5^\circ$ for $H/D = 0.316$), so long as stall was not present. This showed that the performance of the coaxial rotor system (at a prescribed axial separation) is dependent only on the upper and lower rotor pitch difference, independent of thrust level. Figure 30 shows that the effect of separation distance on the optimal performance of the system is not very noticeable for practical operation. It does confirm,

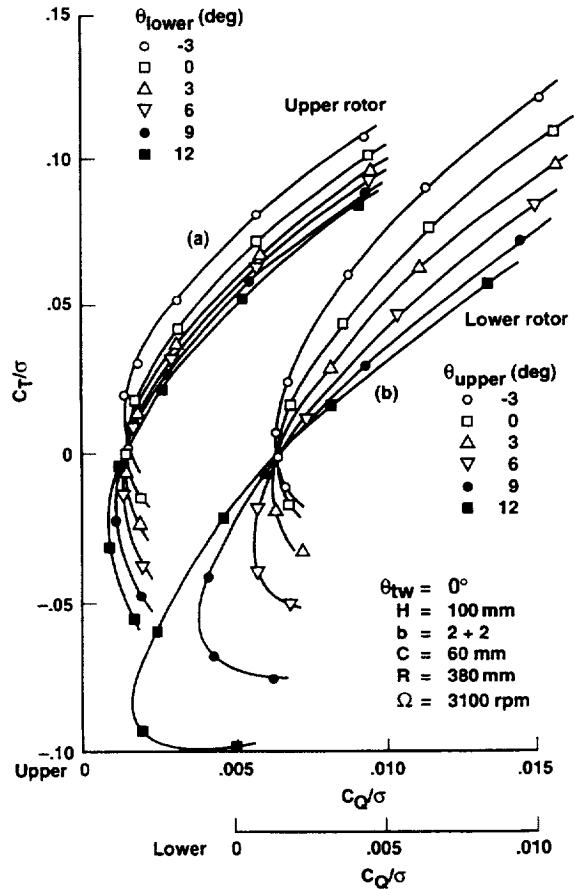


Figure 28. Effect of mutual interaction on rotor performance in hover, $H/D = 0.132$ (ref. 40).

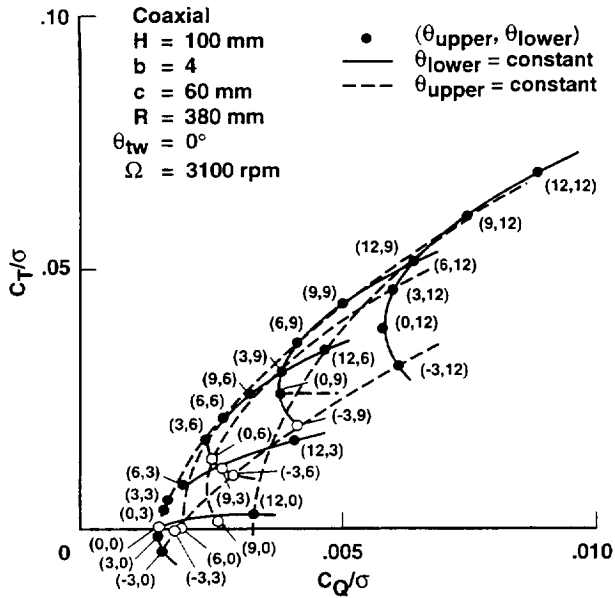


Figure 29. System hover performance, $H/D = 0.132$ (ref. 40).

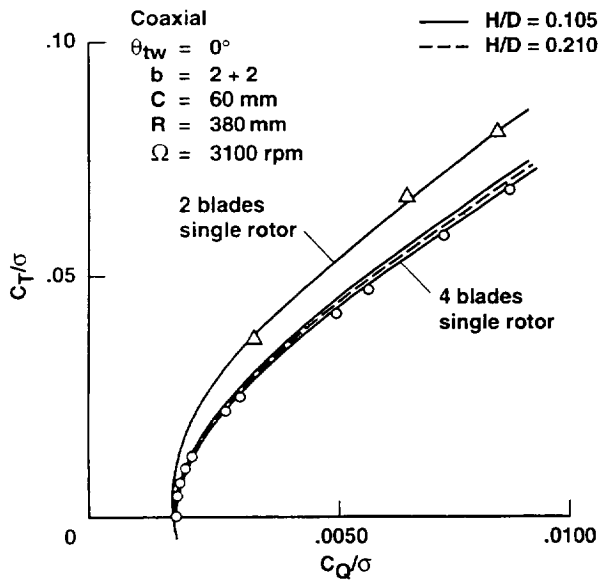


Figure 30. Effect of separation distance on the optimal performance of the hovering system (ref. 40).

however, that the optimal hover performance of the coaxial rotor is better than the hover performance of a single four-bladed rotor for all separation distances (approximately 6% less power for a given thrust at $H/D = 0.210$). This is attributed to an appropriate choice of pitch angle to improve the rotor flow field.

By examining all of the experimental data, it was found that the thrust and torque sharing ratios were constant for

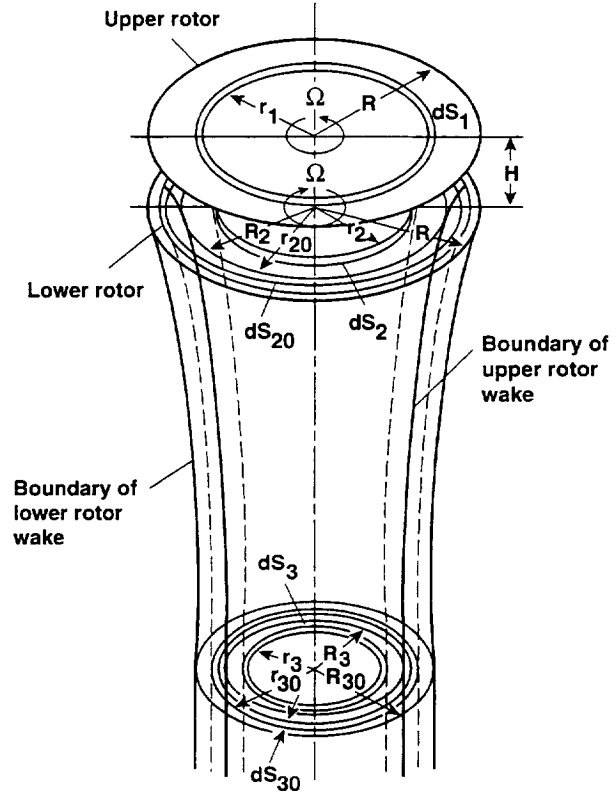


Figure 31. Wake model for a coaxial rotor in hover (refs. 41 and 43).

differential pitch angles equal to those obtained above for optimal performance. These pitch settings (and hence optimal performance) always gave a torque balance between the two rotors that was independent of thrust level and separation. The thrust sharing ratio at these conditions was also independent of the thrust level, but was dependent on separation distance.

Theoretical models for the performance prediction of a coaxial rotor in hover were developed by Nagashima and Nakashi (refs. 41, 43) using both actuator disc and free-wake analyses. Figure 31 shows the rotors modeled as actuator discs with their respective wakes that take account of contraction and swirl. The inner part of the lower rotor (region 2) experiences a downwash from the upper rotor (region 1), while the outer part of the lower rotor (region 20) experiences an upwash. The far wake was designated regions 3 and 30. The rotors are divided into a number of annular elements, across which pressure and swirl are discontinuous. The incremental thrusts at each annular element are obtained in terms of the pressure jumps across the rotors and the swirls in the wakes. This leads to equations (A) and (B), which describe the relations between the axial and rotational velocities in the wakes of a hovering coaxial rotor:

$$\frac{w_3}{2} = \left[\frac{\Omega - \frac{1}{2}\omega'_1}{w_1} - \frac{\Omega - \frac{1}{2}\omega_2}{w_3} \right] K_{r1} \quad (A)$$

$$+ \left[\frac{\Omega - \left(\frac{1}{2}\omega'_2 - \omega_2\right)}{w_2} - \frac{\Omega - \left(\frac{1}{2}\omega'_2 - \omega_2\right)}{w_3} \right] K_{r2}$$

$$\frac{w_{3O}}{2} = \left[\frac{\Omega - \frac{1}{2}\omega'_{2O}}{w_{2O}} - \frac{\Omega - \omega_{3O}}{w_{3O}} \right] K_{r2O} \quad (B)$$

where w is the axial velocity of fluid, ω is the swirl velocity of fluid, Ω is the rotational speed of rotors, and K_{r_i} is the circulation of fluid at each station in the wake. Primed quantities denote values at the lower surface of their respective rotor.

Thrust and power coefficients are expressed as:

$$C_T = \frac{1}{8} \lambda_3^2 (1 + \tau) + \varepsilon_1$$

$$C_P = \frac{C_T}{1 + \tau} \left\{ 2\lambda_1 + (\tau - \alpha) \frac{\lambda_{3O}}{2} \right\} + \varepsilon_2$$

where

$$C_T = \frac{T}{\rho \pi R^2 (\Omega R)^2}, \quad C_P = \frac{\bar{P}}{\pi \rho R^2 (\Omega R)^3}$$

(\bar{P} = total induced power)

$$\lambda_1 = \frac{w_1}{\Omega R}, \quad \lambda_2 = \frac{w_2}{\Omega R}, \quad \lambda_3 = \frac{w_3}{\Omega R},$$

$$\lambda_{3O} = \frac{w_{3O}}{\Omega R} = 2\lambda_{2O}$$

where α is the contraction ratio of the upper rotor wake at the lower rotor and τ is the thrust sharing ratio = T_{low}/T_{upp} . The thrust and power losses caused by rotation of the fluid in the wakes (ε_1 and ε_2 , respectively) are ignored as they are considered to be of small order.

One interesting aspect of this work is the modeling of the mutual interactions between wakes and rotors, which are included by defining nondimensional axial velocities at each rotor as:

$$\lambda_2 = \lambda_l + k\lambda_u, \quad \lambda_{2O} = \lambda_l + k''\lambda_u$$

λ_u and λ_l are nondimensional induced velocities of the upper and lower rotor defined by:

$$\lambda_u = \sqrt{\frac{C_T}{1 + \tau}}, \quad \lambda_l = \sqrt{\frac{\tau C_T}{1 + \tau}}$$

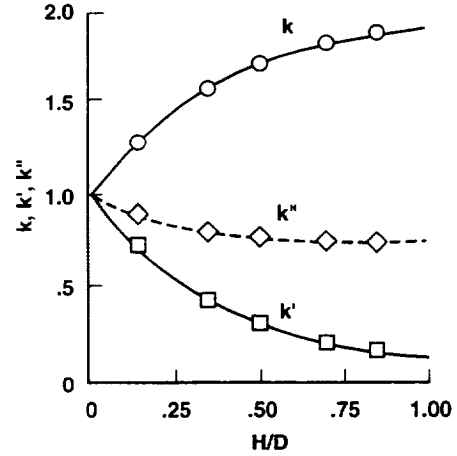


Figure 32. Rotor mutual interaction factors, developed from references 41 and 43.

The influence factors k , k' and k'' are functions of the axial spacing and are denoted by:

$$k = 1 + \frac{2H/D}{\sqrt{1 + 4H^2/D^2}}, \quad k' = 2 - k, \quad k'' = \frac{1}{\sqrt{k}}$$

and are shown in figure 32. Factors k and k' were derived from the potential theory for a uniformly loaded actuator disc (ref. 48), whereas k'' was derived from experimental results (ref. 39) to adequately model the upwash effects of the contracted upper rotor wake on the outer part of the lower one. As can be seen, λ_1 decreases with increasing spacing as there is less induction from the lower rotor; λ_2 increases with increasing spacing, since the contraction of the upper rotor wake causes the axial velocity to increase, which then impacts the lower rotor; and λ_{2O} decreases with increasing spacing, since the amount of upwash decreases with increasing spacing.

The optimal performance was then "formulated as a calculus of variation problem with movable boundaries to determine the far wake axial and swirl velocities distributions which minimize the total induced power, subject to a given total thrust and constraints given by equations (A and B)." The optimal performance was determined by applying:

$$\frac{\partial}{\partial \tau} \left(\frac{C_P}{C_T^{3/2}} \right) = 0$$

These "optimal conditions" led to the axial velocities in the outer wake, w_{2O} and w_{3O} , being exactly zero at any separation distance. This implies that the wake of the lower rotor will be coincident with that of the contracted upper rotor wake, and the outer part of the lower rotor will operate as if it were in autorotation. Figure 33 shows

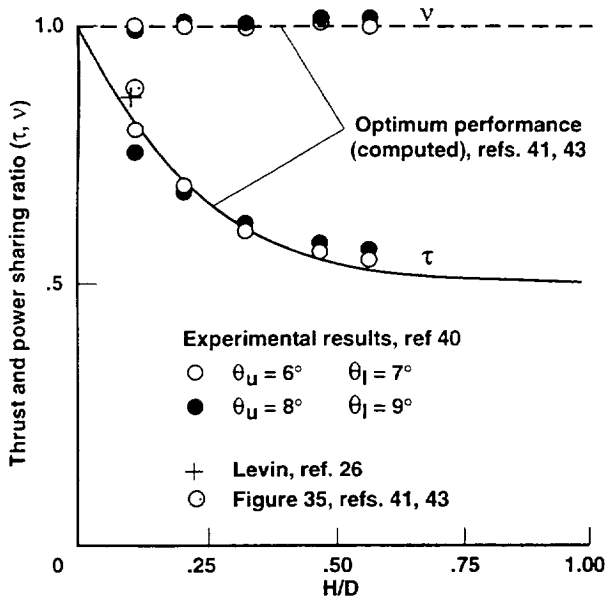


Figure 33. Effect of axial spacing on optimum thrust and power ratios (refs. 41 and 43).

the computed effects of axial spacing on the optimal thrust and power sharing ratios, and these effects are compared with experimental results (ref. 40). The experimentally obtained result of A. D. Levin (ref. 26) is also shown in figure 33, and it compares favorably with both the actuator disc and experimental results. Simplified sketches of flow visualization results are shown in figure 34. By observing the traces of smoke particles, it was found that the axial velocity in the tip region of the lower rotor could vary from upwash to downwash depending on the thrust sharing ratio. It was therefore argued that the condition of zero axial velocity at this outer region could be obtained, and that this would equate to optimal operating conditions, as shown in figure 34. This condition would also give a uniform induced velocity distribution in the far wake, which, by the generalized momentum theory, would equate to minimal induced power of the system. However, in practice, such a uniform velocity distribution would not be obtainable.

Nagashima et al. (refs. 41 and 43) noted that the optimal thrust sharing ratio was roughly equal to the contraction ratio of the upper rotor wake at the lower rotor.

In order to treat the rotor mutual interactions in more detail, nonlinear vortex theory with a simplified free-wake analysis was applied. The rotor blades were modeled by a lifting line with a uniform circulation distribution, while the wakes consisted of a finite number of discrete circular vortices. Wake geometries for a

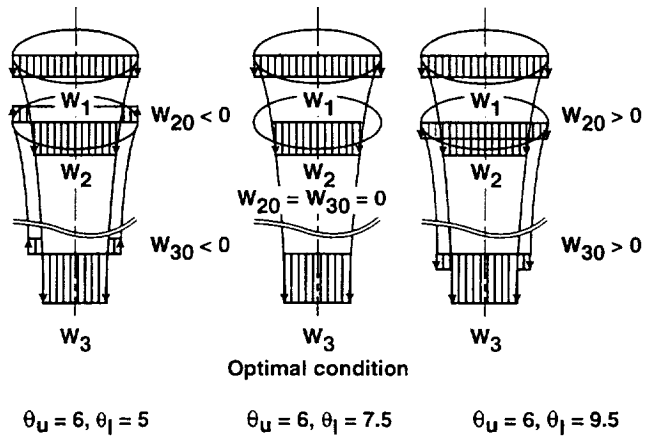


Figure 34. Simplified sketches of typical flow visualization results (ref. 43).

coaxial rotor with a diameter of 6.56 ft (2 m) and chord of 0.26 ft (0.08 m) at 500 rpm were calculated for several separation distances, all for the same total thrust. Figure 35 is the "near optimum" condition, with the wake trajectories almost coincident, power sharing ratio near unity, and thrust sharing ratio of 0.88 (which is close to the contraction ratio of the upper rotor at the lower rotor). This calculated value is also plotted in figure 33 and found to be in good agreement. Also notice how the movement of the tip vortices of the lower rotor are predominantly radial in nature.

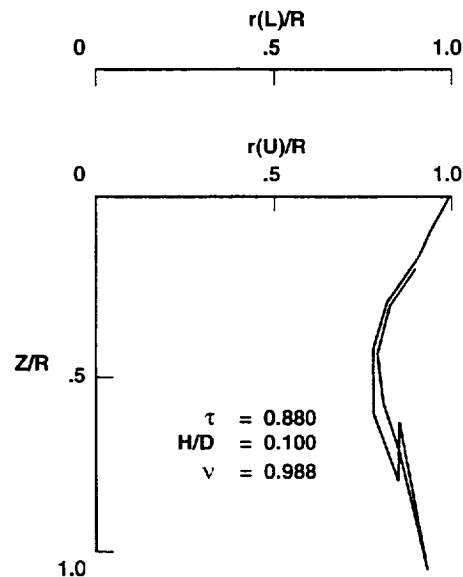


Figure 35. An example of computed wake geometry at $H/D = 0.10$ (refs. 41 and 43).

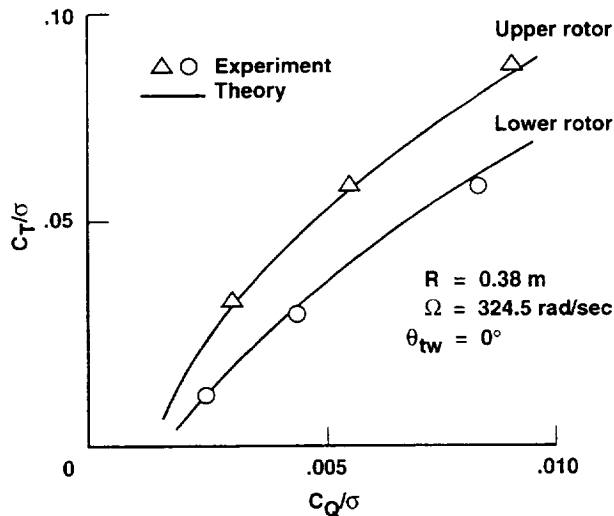


Figure 36. Comparison of theoretical (ref. 42) and experimental (ref. 39) static-thrust performance, $H/D = 0.13$.

Local momentum theory with a modified Landgrebe wake (ref. 51) was applied to a coaxial rotor in hover by Saito and Azuma (ref. 42). The influence of the lower rotor on the upper rotor was modeled using the charts of reference 48; for a given separation distance, these charts yielded the extra induced velocity through the upper rotor from the lower rotor. Annular vortices were used to model the effect of upwash on both rotors. Figure 36 shows that the results of Saito and Azuma correlated well with the experimental results of Nagashima et al. (ref. 39).

Forward Flight

A study of the aerodynamics of a coaxial rotor system in forward flight was made in 1977 by Shinohara (ref. 38) using the same experimental apparatus as in reference 39 with both coaxial and single rotors. Figure 37 graphically shows the large influence that the upper rotor has on the lower. Increasing advance ratio causes the upper rotor wake to be "swept back." This results in more of the lower rotor being exposed to clean air, which leads to better performance. Figure 38 shows that the optimal differential pitch setting decreased from hover by about 0.5° with both increasing advance ratio and spacing. Figure 39 compares a coaxial rotor system at various spacings with a two- and four-bladed (equivalent solidity) single rotor in hover and at $\mu = 0.16$. The improvement in coaxial rotor performance over the equivalent solidity, single rotor is more evident with increasing advance ratio (due to the convection of the tip vortices). Again, this is

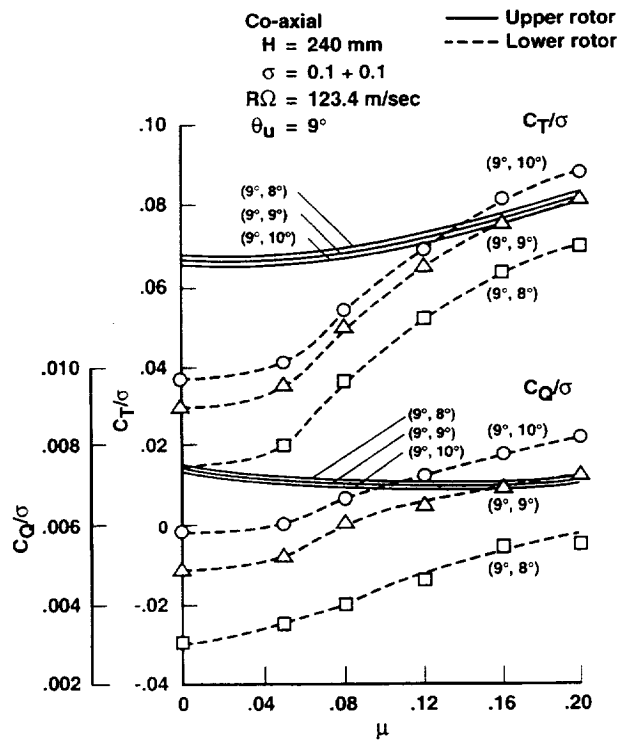


Figure 37. Performance characteristics as a function of advance ratio, showing large influences of upper rotor on lower, $H/D = 0.316$ (ref. 38).

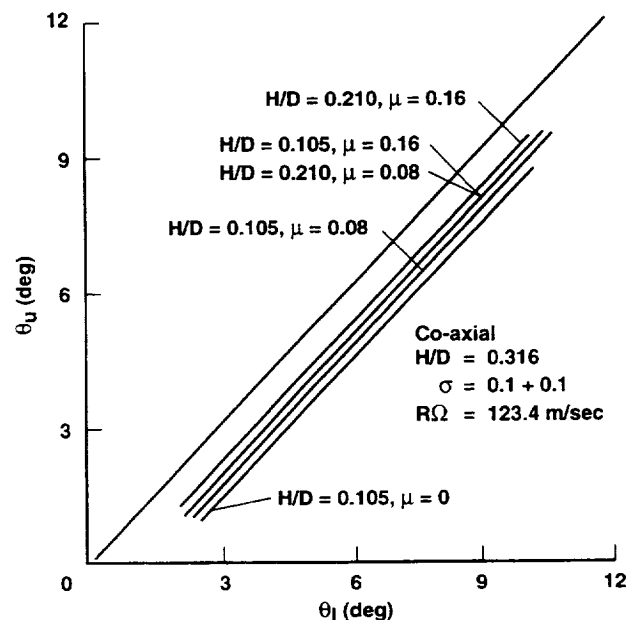


Figure 38. Comparison of optimum pitch angle differences (ref. 38).

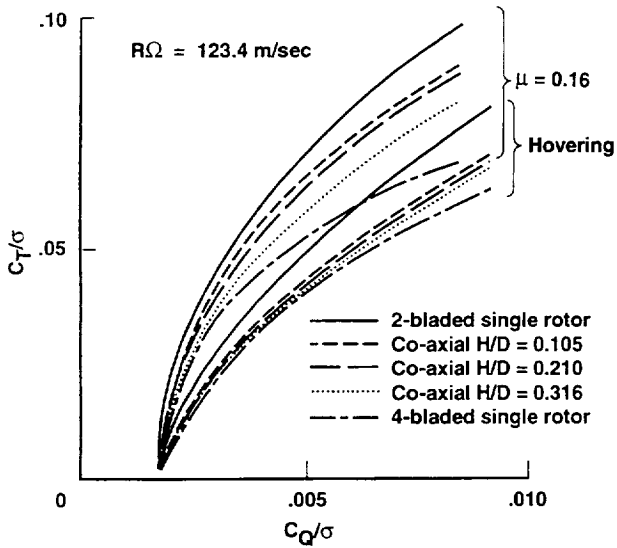


Figure 39. Optimum coaxial vs. single rotor performances in hover and forward flight (ref. 38).

in disagreement with the results of Dingledein (ref. 4), but does follow the same trend as the ABC (ref. 8).

Saito and Azuma (ref. 42) also applied their local momentum theory approach to forward flight. The hovering theory was modified by considering the wakes to be skewed vortex cylinders with no wake contraction. Their calculated performances agreed well with the experimental results of Shinohara (ref. 38) at an advance ratio of 0.16 for $H/D = 0.210$ and 0.316 . However, there was a significant overprediction of performance for $H/D = 0.105$ (approximately 7% less power for a given thrust), which was attributed to disregarding the wake contraction.

Research in the United Kingdom

In the mid-1970s, Westland Helicopters Ltd. began experimenting with small axisymmetric remotely controlled coaxial helicopters. The first of these was named Mote, and its handling qualities were outlined in reference 47. Mote had a teetering rotor of 5 ft (1.52 m) diameter, tip speed of 236 ft/sec (72 m/sec), and total mass of 33 lb (15 kgm).

Andrew (refs. 44 and 45) conducted an experimental and theoretical investigation of coaxial rotor aerodynamics at the University of Southampton in the early 1980s using a stripped-down version of Mote. The model was tested in both hover and forward flight modes with smoke visualization to observe the tip vortices of each rotor.

The theoretical hover analysis used was called a vortex/momentum/blade-element approach, which was a blade-element/momentum approach with a vortex representation of the tip vortex. The tip vortex wake was discretized into a series of straight line filaments that were either made to follow the prescribed paths of reference 51, or were “relaxed” using a free-wake option. Semiempirical equations were developed for the initial viscous vortex core size and maximum swirl velocities. Hover theory was based on figure 40, in which the tip wake from the upper rotor impinges on the lower rotor at a radial distance R_c . The total induced velocity at any position r on the upper rotor ($w_{iu}(r)$) was composed of several components:

$$w_{iu}(r) = w_{mu}(r) + w_{vu}(r) + w_{vl}(r) ; \quad 0 < r < R_u$$

where

$w_{mu}(r)$ = induced velocity from strip theory

$w_{vu}(r)$ = induced velocity from upper tip vortex wake

$w_{vl}(r)$ = induced velocity from lower tip vortex wake

The outer part of the lower rotor which takes in clean air had an inflow given by:

$$w_{il}(r'') = w_{ml}(r'') + w_{vl}(r'') + w_{vu}(r'') ; \quad R_c < r'' < R_l$$

where

$w_{ml}(r'')$ = induced velocity from strip theory

$w_{vl}(r'')$ = induced velocity from lower tip vortex wake

$w_{vu}(r'')$ = induced velocity from upper tip vortex wake

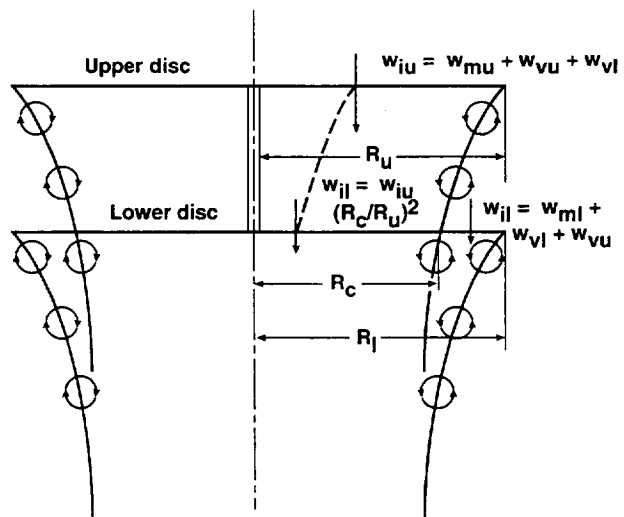


Figure 40. Hover theory (ref. 45).

The inflow for the lower rotor, which was immersed in the wake from the upper rotor, was:

$$w_{il}(r') = w_{iu}(r) (R_c/R_u)^2 ; \quad 0 < r' < R_c \quad (C)$$

where $r' = r (R_c/R_u)$ from continuity. This, however, failed to take into account the effect of the pressure jump across the lower rotor, which results from the lift generated on the lower rotor. An elemental stream tube that passed through both rotors was considered, with radius r on the upper rotor and radius r' on the lower rotor. This stream tube generated a thrust $dT(r)$, where:

$$dT(r) = 4\pi r [w_v(r) + w_{im}(r)] w_{im}(r) dr \quad (D)$$

where $w_v(r)$ was the induced velocity from both upper and lower tip vortex wakes combined, and $w_{im}(r)$ was the strip theory value for the induced velocity.

But:

$$dT(r) = dT_u(r) + dT_l(r') \quad (E)$$

Therefore, equating (D) with (E), and using (C), yielded a quadratic in $w_{im}(r)$, which was solved for. Hence, the inflow angle (ϕ) at any blade element was evaluated from:

$$\phi(r) = (w_v(r) + w_{im}(r)) / \Omega r$$

A comparison of the experimentally obtained wake trajectories with that of the Landgrebe prescribed wake for a single rotor showed stronger and weaker contraction of the upper and lower wakes, respectively (fig. 41). (Although not shown, it is presumed that this is also accompanied by an increase in axial velocities; this would be in agreement with Russian and Japanese observations.) The prescribed wake was subsequently modified to allow only for an increased axial translation of the upper rotor wake as it traversed the lower rotor (ref. 45). In comparison with experiment, the theory underpredicted the torque for a given thrust, which was attributed to neglecting the circulation distribution outside the vortex core in the vortex induced velocity calculations. The theory was used to predict the performance of a four-bladed single rotor with a solidity equivalent to Mote's. In this case, for a given thrust, the coaxial absorbed approximately 5% less power than the equivalent single rotor. These increases were attributed to:

1. The contraction of the upper wake of a coaxial, which allowed clean air with a slight upwash to be taken by the outboard sections of the lower rotor. Consequently, the effective coaxial disc area increases with a corresponding reduction in induced power.
2. The vertical spacing of the rotors in the coaxial layout, which lessened the severity of the total vortex induced downwash, especially on the upper rotor.

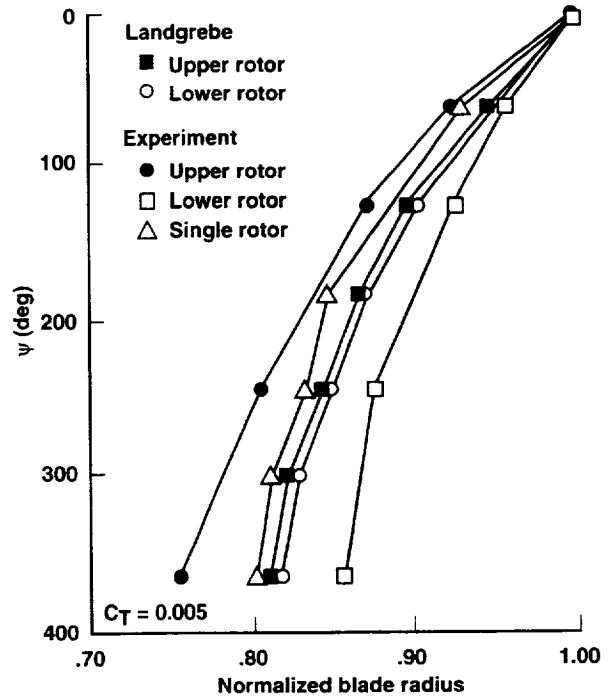


Figure 41. Comparison of Landgrebe and coaxial rotor wake limits (ref. 44).

3. "Swirl recovery," which was considered a secondary effect for low disc loadings.

Forward flight theory employed the classical, skewed cylindrical wake at high advance ratios, or a free-wake analysis at low advance ratios (ref. 45). The effect of the tip vortex was approximated by incorporating the vortex induced velocity through the center of the disc. For the classical, skewed-wake option, a further allowance was made for the influence of the tip vortex wake on a specified blade element by evaluating the downwash at that element. Figures 42 and 43 show comparisons between theory and experimental forward flight Mote data at a constant thrust coefficient of 0.008 and advance ratio of 0.174, respectively. In both cases, the classical wake option was found adequate for estimating the overall performance of Mote.

An optimization study of the coaxial rotor in hover was also undertaken using the developed theory (ref. 45). Three parameters were identified that would increase the efficiency (thrust generated per unit power) of the coaxial over an equivalent solidity, single rotor:

1. Vertical spacing. The greatest gains were made up to $H/D = 0.05$; thereafter, no "practical" gains resulted with increasing separation distance.

2. A reduction in upper rotor radius. "There is a trade off between the increase in induced power of the upper rotor with a reduction in the upper rotor radius, and the enhanced performance of the lower rotor as proportionately more disc is exposed to clean air. The most promising results were obtained for an 8% reduction in upper rotor radius."
3. An increase in blade aspect ratio.

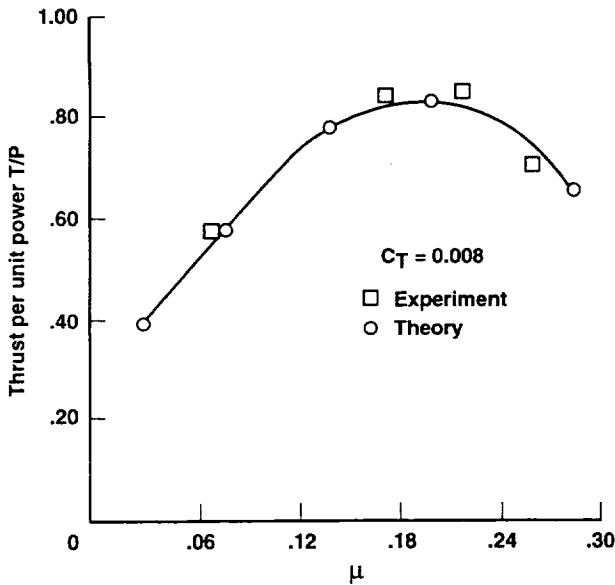


Figure 42. Comparison of experimental and theoretical Mote forward flight performance (ref. 45).

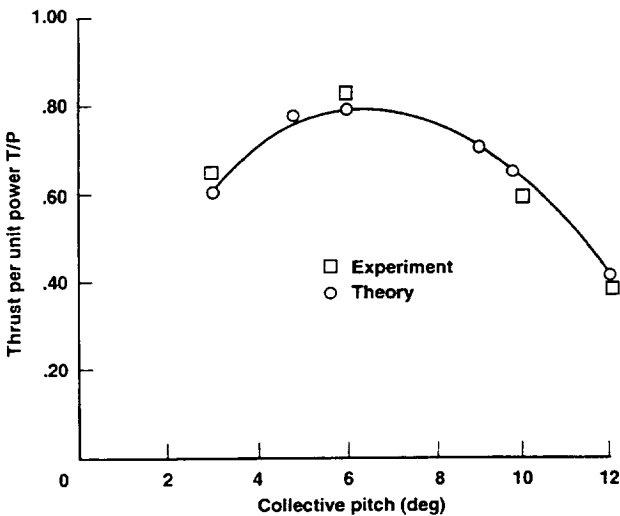


Figure 43. Comparison of experimental and theoretical Mote performance, $\mu = 0.174$ (ref. 45).

Research in Germany

Zimmer (ref. 46) developed a method described as a curved lifting-line/vortex wake/blade-element/momentum concept. The rotor blades were divided into two-dimensional blade elements that had the curved lifting line method applied to them. The shed vortices from each element were accounted for a short distance behind each station, while the trailed vortices were carried on downstream. The radial contraction of the tip vortices was specified for the first and second rotors using information from references 42 and 44. The Biot-Savart law was applied at every time step to obtain the induced flow for points in the flow field, including the velocity through rotors 1 and 2. The downwash distributions were corrected for wake truncation errors in two ways. The downwash correction in the plane of the second rotor was such that the downwash distribution of the first rotor was increased according to continuity. For the momentary blade position on the second rotor, the actual downwash correction was interpolated. The downwash distributions were corrected in such a way that the rotor thrust was compatible with axial momentum theory. After all the necessary results were converged and found in every time step, the overall rotor coefficients were determined.

Results were presented for both the single and coaxial rotors from Harrington's experiments (ref. 3). Initial results for the coaxial rotor underpredicted performance at high values of C_T (curve B in fig. 44). A higher mass flow through the influence area IA than through the upper rotor was subsequently assumed to better represent the measurements in the high thrust cases (curve A).

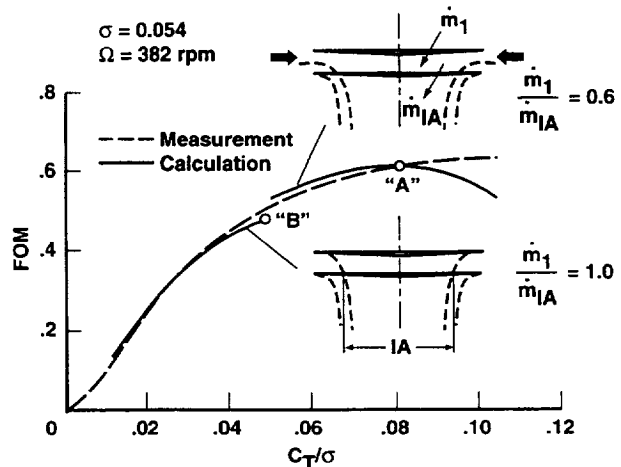


Figure 44. Discontinuous theory vs. experimental results of references 3 and 46.

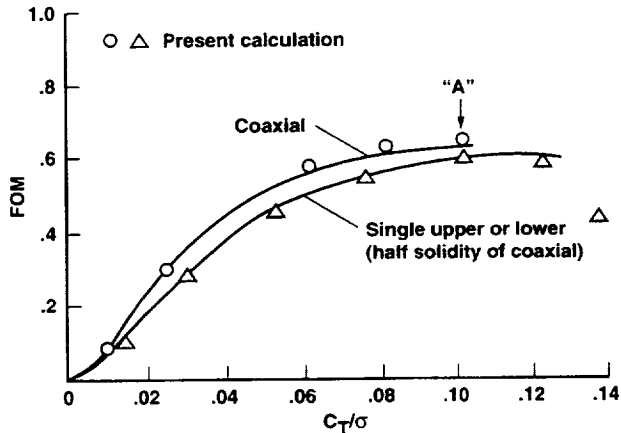


Figure 45. Static-thrust prediction incorporating automatic contraction of tip vortices (private correspondence).

However, curves A and B form a discontinuous performance function, which is not desired. Zimmer (ref. 46) concluded that a variable contraction of the tip vortex of the first rotor should be incorporated into his model.

In a subsequent correspondence (unreferenced), Zimmer stated that the automatic contraction of the tip vortices had been incorporated into his analysis. Figure 45 (when compared with fig. 44) shows that the method does well in following the experimental figure of merit curve, and only slightly overpredicts performance at high thrust loading. The calculated wake geometry at point A showed a relative convergence between upper and lower tip vortices in agreement with Nagashima's results (ref. 39).

Conclusions

A survey of coaxial rotor aerodynamics in both hover and forward flight has been conducted from both theoretical and experimental viewpoints. The often used equivalent solidity, single-rotor approach to modeling coaxial rotors in hover has been shown to require approximately 5% more power for a given thrust. It therefore serves as a good first approximation to the hovering performance of a coaxial rotor. For an improved theory, one must understand the aerodynamic intricacies of the coaxial rotor. Forward flight prediction using the equivalent solidity approach has been shown to produce very different answers than experiment (Dingledein (ref. 4) and ABC (ref. 8)).

A hovering coaxial rotor has several distinctive characteristics. First, it has been observed that the wake from the upper rotor contracts inward and convects downward at a faster rate than if the rotor were in isolation. The lower rotor also experiences a faster axial

convection rate, with an ill-defined radial contraction.

Thus, any attempt to model the upper or lower rotor wakes with a Landgrebe-type prescribed wake (based on a single, isolated rotor) must use different convection and contraction rates, as in references 41 and 43. Altering the separation distance (for an approximately fixed total thrust) alters only the thrust sharing ratios between the two rotors (for a torque-balanced configuration); figure 30 shows that varying the separation distance has little practical use by itself.

The contraction of the upper rotor wake allows clean air with a slight upwash to be taken by the outboard section of the lower rotor. Consequently, the effective disc area of the coaxial rotor in hover increases with a corresponding decrease in the effective disc loading and induced power. There is also Nagashima's observation (ref. 39) that there is a beneficial effect to having the two rotors interact, in that the spatial placement of the tip vortices in the wake can influence the performance of the system. To some extent, these statements explain the increase in performance of a coaxial over an equivalent single rotor in hover (roughly 5% less power for same given thrust).

It was also observed (ref. 39) that the rotor with higher collective setting "dominates" the system flow field, meaning that the wake structure associated with that rotor is the most prevalent. Optimal performance is claimed to be a special case when neither rotor dominates and the vortices from both rotors are evenly spaced in the wake (affirmed by performance results (ref. 40)). This optimal performance condition dictates that there be a torque balance between the two rotors (a fact substantiated by Harrington's experiments with non-torque-balanced configurations and corresponding increases in power). Except for hovering turns, a coaxial rotor in hover usually requires a torque balance, and so may unwittingly operate in this optimal condition (more work is required to substantiate this theory).

Swirl recovery in the wake (although mentioned often as contributing to the coaxial's performance) becomes more important as the disc loading increases. For most operational coaxial helicopters, however, swirl recovery is a secondary effect.

The great advantage of a coaxial helicopter in hover is its lack of a tail rotor and the power which that would require. As a result, coaxial helicopters are good choices for hovering platforms.

In forward flight experiments, the coaxial rotor required less power than an equivalent solidity single rotor (up to moderate advance ratios) (ref. 38). This was mainly due to the reduction in induced power, which was caused by the "sweeping back" of the wakes and the reduction of

upper rotor interference on the lower rotor. The “hub drag” associated with the coaxial configuration will eventually cause the parasite drag to dominate at high advance ratios, thus giving the coaxial rotor a higher drag penalty than the equivalent single rotor.

A variety of coaxial rotor theoretical models has been presented. Simple interference models not only include the effect of the upper rotor on the lower, but are also usually adapted to account for the effect of the lower rotor on the upper (refs. 41 and 43). This latter effect decreases appreciably with increasing separation distance. Annular vortices (ref. 42) or empirical results (refs. 41 and 43) can also be used to model the effect of upwash on the outer region of the lower rotor caused by the impinging upper rotor wake. The use of free-wake models (refs. 41 and 43-46) provides “computational flow visualization” of the complex wake structure.

Andrew (ref. 45) presented work on theoretically optimizing the hovering coaxial rotor configuration. He found that vertical spacing gave the greatest gains in performance up to $H/D = 0.05$, with no practical gains thereafter. He also found that there was a “trade off between increase in induced power on the upper rotor with the reduction in upper rotor radius and the enhanced performance of the lower rotor as proportionately more disc is exposed to clean air. Most promising results were obtained for a 8% reduction in upper rotor radius.”

Harrington demonstrated that scale effect plays an important role in coaxial rotor testing (as in any rotor testing). Throughout this report, large differences in Reynolds numbers have been reported, probably resulting in different testing conditions. However, comparisons with equivalent solidity, single rotors were always conducted at the same Reynolds number as for the coaxial test, and all showed a performance increase for the coaxial rotor. An investigation of coaxial rotor performance with Reynolds number is required before drawing any more conclusions.

Finally, a detailed experimental study of the induced velocity flow field of a coaxial rotor system is required in order to advance the sophistication of current theoretical models.

References

1. Lambermont, P.; and Pirie, A.: Helicopters and Autogyros of the World. Cassell & Company Ltd., 1970.
2. Taylor, M.: A balsa-dust technique for air-flow visualization and its application to flow through model helicopter rotors in static thrust. NACA TN-2220, Nov. 1950.
3. Harrington, R. D.: Full-scale-tunnel investigation of the static-thrust performance of a coaxial helicopter rotor. NACA TN-2318, Mar. 1951.
4. Dingledein, R. C.: Wind-tunnel studies of the performance of multirotor configurations. NACA TN-3236, Aug. 1954.
5. Gyrodyne Company of America, Inc.: Summary of Gyrodyne technical background including the coaxial helicopter development, sec. 5, vol. 4, Promotional information, Feb. 1971.
6. United Aircraft Research Laboratories: Experimental investigation of the hovering performance of a coaxial rigid rotor. Report F 410533-1, Jan. 1967.
7. Cheney, M. C., Jr.: The ABC helicopter, J. Am. Helicopter Soc., Oct. 1969.
8. Paglino, V. M.: Forward flight performance of a coaxial rigid rotor. Proceedings of the 27th American Helicopter Society Forum, Washington, D.C., May 1971.
9. Burgess, R. K.: Development of the ABC rotor. Proceedings of the 27th American Helicopter Society Forum, Washington, D.C., May 1971.
10. Halley, D. H.: ABC helicopter stability, control and vibration evaluation on the Princeton dynamic model track. Proceedings of the 29th American Helicopter Society Forum, Washington, D.C., May 1973.
11. Ruddell, A. J.: Advancing blade concept development. Proceedings of the 32nd American Helicopter Society Forum, Washington, D.C., May 1976.
12. Klingloff, R. F.: Rigid coaxial rotor system stability and control characteristics. Proceedings of the 32nd American Helicopter Society Forum, Washington, D.C., May 1976.
13. Arents, D. N.: An assessment of the hover performance of the XH-59A advancing blade concept demonstration helicopter. Report USAAMRDL-TN-25, Eustis Directorate, USAAMRDL, Fort Eustis, Va., May 1977.
14. Abbe, J. T. L.; Blackwell, R. H.; and Jenney, D. S.: Advancing blade concept dynamics. Proceedings of the 33rd American Helicopter Society Forum, Washington, D.C., May 1977.

15. Ruddell, A. J. et al.: Advancing blade concept technology demonstrator. Report USAAVRADCOM-TR-81-D-5, Fort Eustis, Va., Apr. 1977.
16. Young, H. R.; and Simon, D. R.: The advancing blade concept rotor program. AGARD-CP-233, proceedings of the Flight Mechanics Panel Symposium, Ames Research Center, Moffett Field, Calif., May 1977.
17. Phelps, A. E.; and Mineck, R. E.: Aerodynamic characteristics of a counter-rotating, coaxial, hingeless rotor helicopter model with auxiliary propulsion. NASA TM-78705, May 1978.
18. Halley, D. H.; and Knapp, L. G.: ABC development status and design considerations for several military applications. Proceedings of the 36th American Helicopter Society Forum, Washington, D.C., May 1980.
19. Ruddell, A. J.; and Macrino, J. A.: Advancing blade concept high speed development. Proceedings of the 36th American Helicopter Society Forum, Washington, D.C., May 1980.
20. Jenney, D. S.: ABC aircraft development status. Proceedings of the 6th European Rotorcraft and Powered Lift Aircraft Forum, Sept. 1980.
21. Linden, A. W.; and Ruddell, A. J.: An ABC status report. Proceedings of the 37th American Helicopter Society Forum, New Orleans, La., May 1981.
22. Felker, F. F.: Performance and loads data from a wind tunnel test of a full-scale, coaxial, hingeless rotor helicopter. NASA TM-81329, Oct. 1981.
23. Ruddell, A. J.: Advancing blade concept development test program. AIAA/SETP/SFTE/SAE/ITEA/IEEE 1st Flight Testing Conference, Las Vegas, Nev., Nov. 11–13, 1981.
24. Tischenko, M. N.: Soviet helicopter technology. Vertiflite, July–Aug. 1989.
25. Baskin, V. E.; Vil'dgrube, L. S.; Vozhdayev, Y. S.; and Maykapar, G. I.: Theory of the lifting airscrew. NASA TT F-823, Feb. 1976.
26. Vil'dgrube, L. S.: Vertolety, raschet integral'nykh aerodynamicheskikh kharakteristik i letno-mekhanicheskikh danykh (Helicopters—calculations of integral aerodynamic characteristics and flight-mechanics data). Moscow, Mashinostroyeniye, 1977 (in Russian).
27. Antopov, V. F. et al.: Eksperimental'nyye issledovaniya po aerodinamike vertoleta (Experimental research on helicopter aerodynamics). Moscow, Mashinostroyeniye, 1980 (in Russian).
28. Belotserkovskiy, S.; and Loktev, B.: Computer simulation of unsteady flow past lifting rotors of coaxial configuration. Doklady akademii nauk SSSR, vol. 256, no. 4, 1981, pp. 810–814 (in Russian).
29. Volodko, A. M.: Osnovy letnoy ekspluatatsii vertoletov, aerodinamika (Fundamentals of helicopter flight operation, aerodynamics). Izdatel'stvo "Transport," 1984, pp. 3–256 (in Russian).
30. Lambert, M.: The Soviets explain the Ka-32 Helix. Interavia, Aug. 1985.
31. Stepniewski, W. Z.; and Burrowbridge, W. R.: Some Soviet and western simplified helicopter performance prediction methods in comparison with tests. Proceedings of the 12th European Rotorcraft Forum, Sept. 1986.
32. Kasjanikov, V. A.: Coaxial helicopters—current status and future developments. Vertiflite, Sept.–Oct. 1990.
33. Burtsev, B. N.: Aeroelasticity of a coaxial rotor. Proceedings of the 17th European Rotorcraft Forum, Sept. 1991.
34. Anikin, V. A.: Aerodynamic feature of a coaxial rotor helicopter. Proceedings of the 17th European Rotorcraft Forum, Sept. 1991.
35. Velovich, A.: Werewolf warrior. Flight International, Sept. 23–29, 1992.
36. Kvokov, V. N.: Factor analysis of coaxial rotor aerodynamics in hover. Proceedings of the 18th European Rotorcraft Forum, Sept. 1992.
37. Burtsev, B. N.: The coaxial helicopter vibration reduction. Proceedings of the 18th European Rotorcraft Forum, Sept. 1992.
38. Shinohara, K.: Optimum aerodynamic character of the coaxial counter rotating rotor system. Graduation thesis, Koku Hisho Kogaku (Flight Engineering), Helicopter Engineering I, The National Defense Academy, Japan, Feb. 1977 (in Japanese).

39. Nagashima, T.; Shinohara, K.; and Baba, T.: A flow visualization study for the tip vortex geometry of the coaxial counter rotating rotor in hover, Technical note, pp. 442–445, J. of Japan Society for Aeronautics & Space Sciences, vol. 25, no. 284, 1978 (in Japanese).
40. Nagashima, T.; Ouchi, H.; and Sasaki, F.: Optimum performance and load sharing of coaxial rotor in hover. J. of Japan Society for Aeronautics & Space Sciences, pp. 325–333, vol. 26, no. 293, June 1978 (in Japanese).
41. Nagashima, T.; and Nakanishi, K.: Optimum performance and wake geometry of coaxial rotor in hover. Proceedings of the 7th European Rotorcraft and Powered Lift Forum, Paper No. 41, Sept. 1981.
42. Saito, S.; and Azuma, A.: A numerical approach to coaxial rotor aerodynamics. Proceedings of the 7th European Rotorcraft and Powered Lift Forum, Paper No. 42, Sept. 1981.
43. Nagashima, T.; and Nakanishi, K.: Optimum performance and wake geometry of a coaxial rotor in hover. *Vertica*, vol. 7, 1983, pp. 225–239.
44. Andrew, M. J.: Coaxial rotor aerodynamics in hover. *Vertica*, vol. 5, 1981, pp. 163–172.
45. Andrew, M. J.: Coaxial rotor aerodynamics. Ph.D. thesis, Southampton University, England, circa 1981.
46. Zimmer, H.: The aerodynamic calculation of counter rotating coaxial rotors. Proceedings of the 11th European Rotorcraft and Powered Lift Forum, Paper No. 27, Sept. 1985.
47. Faulkner, A. J.; and Simons, I. A.: The remotely piloted helicopter. *Vertica*, vol. 1, 1977, pp. 231–238.
48. Castles, W.; and de Leeuw, J. H.: The normal component of the induced velocity in the vicinity of a lifting rotor and some examples of its application. NACA TN-2912, Mar. 1953.
49. Sweet, G. E.: Static-stability measurements of a stand-on type helicopter with rigid blades, including a comparison with theory. NASA TN D-189, Feb. 1960.
50. Landgrebe, A. J.; and Bellinger, E. D.: Experimental investigation of model variable-geometry and ogee tip rotors. Proceedings of the 29th American Helicopter Society Forum, Washington, D.C., May 1973.
51. Landgrebe, A. J.: An analytical and experimental investigation of helicopter rotor hover performance and wake geometry characteristics. USAAMRDL Tech. Rept. 71-24, Eustis Directorate, USAAMRDL, Fort Eustis, Va., June 1971.

REPORT DOCUMENTATION PAGEForm Approved
OMB No. 0704-0188

Public reporting burden for this collection of information is estimated to average 1 hour per response, including the time for reviewing instructions, searching existing data sources, gathering and maintaining the data needed, and completing and reviewing the collection of information. Send comments regarding this burden estimate or any other aspect of this collection of information, including suggestions for reducing this burden, to Washington Headquarters Services, Directorate for Information Operations and Reports, 1215 Jefferson Davis Highway, Suite 1204, Arlington, VA 22202-4302, and to the Office of Management and Budget, Paperwork Reduction Project (0704-0188), Washington, DC 20503.

1. AGENCY USE ONLY (Leave blank)		2. REPORT DATE March 1997	3. REPORT TYPE AND DATES COVERED Technical Paper	
4. TITLE AND SUBTITLE A Survey of Theoretical and Experimental Coaxial Rotor Aerodynamic Research			5. FUNDING NUMBERS 522-31-12 522-41-22	
6. AUTHOR(S) Colin P. Coleman				
7. PERFORMING ORGANIZATION NAME(S) AND ADDRESS(ES) Ames Research Center Moffett Field, CA 94035-1000			8. PERFORMING ORGANIZATION REPORT NUMBER A-975555	
9. SPONSORING/MONITORING AGENCY NAME(S) AND ADDRESS(ES) National Aeronautics and Space Administration Washington, DC 20546-0001			10. SPONSORING/MONITORING AGENCY REPORT NUMBER NASA TP-3675	
11. SUPPLEMENTARY NOTES Point of Contact: Colin P. Coleman, Ames Research Center, MS 260-1, Moffett Field, CA 94035-1000 (415) 604-0613				
12a. DISTRIBUTION/AVAILABILITY STATEMENT Unclassified — Unlimited Subject Category 02			12b. DISTRIBUTION CODE	
13. ABSTRACT (Maximum 200 words) The recent appearance of the Kamov Ka-50 helicopter and the application of coaxial rotors to unmanned aerial vehicles have renewed international interest in the coaxial rotor configuration. This report addresses the aerodynamic issues peculiar to coaxial rotors by surveying American, Russian, Japanese, British, and German research. (Herein, "coaxial rotors" refers to helicopter, not propeller, rotors. The intermeshing rotor system was not investigated.) Issues addressed are separation distance, load sharing between rotors, wake structure, solidity effects, swirl recovery, and the effects of having no tail rotor. A general summary of the coaxial rotor configuration explores the configuration's advantages and applications.				
14. SUBJECT TERMS Coaxial, Rotor, Aerodynamic			15. NUMBER OF PAGES 32	
			16. PRICE CODE A03	
17. SECURITY CLASSIFICATION OF REPORT Unclassified	18. SECURITY CLASSIFICATION OF THIS PAGE Unclassified	19. SECURITY CLASSIFICATION OF ABSTRACT	20. LIMITATION OF ABSTRACT	